Volume 20
Number 14
14 April 2022
Pages 2733-2982

Organic & Biomolecular Chemistry

rsc.li/obc

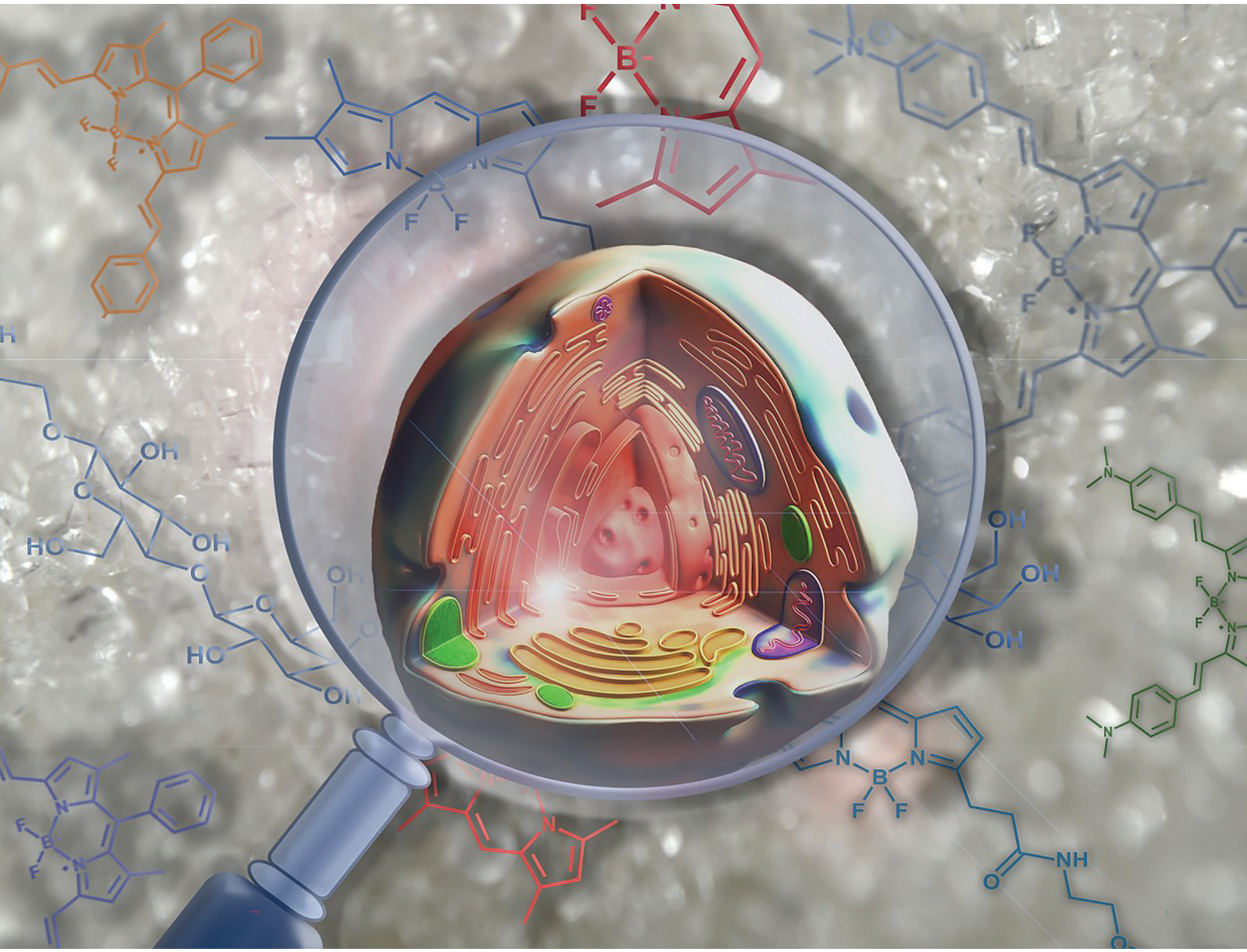

ISSN 1477-0520

ROYAL SOCIETY OF CHEMISTRY

REVIEW ARTICLE

Sebastiano Campagna, Fausto Puntoriero, Paola Bonaccorsi *et al.*

Bodipy-carbohydrate systems: synthesis and bio-applications

Organic & Biomolecular Chemistry

ROYAL SOCIETY OF CHEMISTRY

REVIEW

View Article Online
View Journal | View Issue

Cite this: *Org. Biomol. Chem.*, 2022, **20**, 2742

Bodipy-carbohydrate systems: synthesis and bio-applications

Anna Barattucci, Chiara M. A. Gangemi, Antonio Santoro, Sebastiano Campagna, * Fausto Puntoriero * and Paola Bonaccorsi *

Received 21st December 2021,
Accepted 2nd February 2022

DOI: 10.1039/d1ob02459k

rsc.li/obc

Luminescent BODIPY-sugar probes have stimulated the attention of researchers for the potential applications of such molecular systems in bio-imaging. The presence of carbohydrate units confers unique structural and biological features, beside enhancement of water solubility and polarity. On the other hand, BODIPY (BOronDiPYrromethene) derivatives represent eclectic and functional luminescent molecules because of their outstanding photophysical properties. This article provides a review on the synthesis and applications of BODIPY-linked glycosyl probes in which the labelling of complex carbohydrates with BODIPY allowed the disclosing of their *in vivo* behaviour or where the sugar constitutes a recognition element for specific targeting probes, or, finally, in which the stereochemical characteristics of the carbohydrate hydroxyl groups play as structural elements for assembling more than one photoactive subunit, resulting in functional supramolecular molecules with modulable properties. We describe the methods we have used to construct various multiBODIPY molecular systems capable of functioning as artificial antennas exhibiting extremely efficient and fast photo-induced energy transfer. Some of these systems have been designed to allow the modulation of energy transfer efficiency and emission color, and intensity dependent on their position within a biological matrix. Finally, future perspectives for such BODIPY-based functional supramolecular sugar systems are also highlighted.

Introduction

Carbohydrates are among the most structurally complex and, for this reason, challenge macromolecules widespread in the biological world. Compared with nucleic acids and proteins, they can form linear or branched structures where the building blocks of the chain, the monosaccharides, can join together through the "almost" equivalent four hydroxyl groups and the anomeric hemiacetal hydroxyl group, that possesses a dual stereochemical feature. In nature, two identical monosaccharides can form as many as eleven different disaccharides,[1,2] while two α-amino acids can originate four α-dipeptides, at most. In a very short glycide sequence an immense wealth of biological information is therefore enclosed and the conveyed messages differ according to the type of monomer, the differences in the bonds, the presence and the degree of ramifications and, finally, the presence of substituents different from the hydroxyl groups. This stereochemical and structural diversity provides to Nature a tremendous number of opportunities in differentiating the role of carbohydrates in biologically important events,[3] and to the chemists a challenge to deepen the knowledge of such role or use them in the construction of complex molecular architectures.[4–8]

Luminescence has constituted a tool for an inside journey into the complex world of carbohydrates, for the relative simplicity and sensibility of its techniques. The first and most common usage of luminescence is the labelling of glycans with fluorescent probes to study carbohydrate structures and their interactions in biological systems. The choice of the right probe ensures a great sensitivity in detecting probe-labelled macromolecules such as glycolipids or glycoproteins to disclose their *in vivo* behaviour but, on the other hand, the concern remains that, in these studies, covalently-linked luminophores can lead to changes in the overall property of the glycan and results must be interpreted with great care. In recent years efforts have been directed towards the use of fluorescent glycoconjugate as small targeting probes. The presence of a carbohydrate unit into the luminescent probes has demonstrated to be useful not only on improving its polarity and solubility in aqueous media but also on getting straight to the target "to hit", becoming the sugar a structural recognition element of the probe. There is a third application which justifies the liaison between fluorescence and carbohydrates: due to various unique structural features that carbohydrates possess, such as the well-defined stereochemistry and the presence of transformable hydroxyl group, they have been intro-

Dipartimento di Scienze Chimiche, Biologiche, Farmaceutiche ed Ambientali, Università di Messina, Via F. Stagno d'Alcontres 31, 98166 Messina, Italy.
E-mail: campagna@unime.it, fpuntoriero@unime.it, paola.bonaccorsi@unime.it

duced as scaffolds in the design of functional materials for specific applications.

The careful choice of the fluorophore and the attachment probe/sugar chemistry have stimulated the proliferation of articles on fluorescent glycoconjugates, with an increase employment of BODIPY as the fluorophore of choice.[9–14]

Actually, BODIPY dyes are excellent substrates for the development of functional fluorescent systems for their high photostability, high luminescence quantum yield and excited state lifetimes in the ns timescale.[15–22] Moreover, the emissive properties of BODIPY can be modulated by appropriate substitutions on its skeleton and appropriately controlled by photoinduced energy or electron transfer in multicomponent systems.[23–30] However, due to its structure, BODIPY-core is highly hydrophobic, which makes it often not applicable in aqueous systems and biological samples. Therefore, conjugation with sugar moieties could help in increasing the hydrophilicity of these kind of systems.

The present review will focus on two main issues: (i) the design, synthesis and applications of BODIPY-tagged glycoconjugates, with particular regards to the labelling of carbohydrates with BODIPY and to the synthesis of BODIPY-linked glycosyl probes; and (ii) the synthesis and applications of BODIPYs grafted on a carbohydrate platform. In this context, we will discuss our synthetic strategies, the observed photophysical properties and the future perspectives for their application in bio-imaging.

BODIPY-labelling of glycosydes

The labelling of biomolecules with fluorescent tags, such as BODIPY, is one of the oldest and applied tools for studying the location and trafficking of single components in complex biological systems using fluorescence techniques. Among the BODIPY-labelled biopolymers, proteins and nucleic acids have been the first to be studied. The challenging world of BODIPY-labelled glycosides was argument of research further on, due to the structural complexity of carbohydrates and the diversity of their linkages.

Glycosphingolipids (GSLs) are distributed throughout animal, plant, and microbial cells, within which they play various roles in biological processes. To understand the role of glycans in modulating lipids it is important to identify their structural organization and the molecular context of these oligosaccharides, to study their metabolism and their activities in normal and disease cell types.

Fluorescent labelling of both endogenous and synthetic glycolipids has provided the right tool to work out these demanding tasks, as matter of fact, today BODIPY conjugates with ceramide, such as cerebrosides (**7** and **8** in Scheme 1), globosides (**9** in Scheme 1) or gangliosides (**10** in Scheme 1), are commercially available and used to study the transport and metabolism of sphingolipids and their role in the Golgi apparatus. From a synthetic point of view, these probes are commonly prepared, as described in literature,[31–34] by *N*-acylation of an opportune commercial glycosyl-sphingosine (**1–4** in Scheme 1) (usually the natural (2*S*,3*R*)-D-*erythro*-sphingosine) with commercial 5-(5,7-aminoundecanoic acid dimethyl-BODIPY)-1 propanoic acid **5a**, 5-(5,7-aminoundecanoic acid dimethyl-BODIPY)-1 pentanoic acid **5b**, or their *N*-hydroxy succinimide ester analogues **6a,b** (Scheme 1).

To gain access to quantitative information on GSLs in various samples obtained from cultured cells, grown under different conditions, a simple and efficient strategy for the differential analysis of multiple GSL samples was developed by MS/MS technique, using isobaric tags for relative and absolute quantitation (iTRAQ).[35] LacSphy **3** (depicted in Scheme 1) was linked to fluorescent BODIPYs, opportunely functionalized to incorporate iTRAQ, using 4-(4,6-dimethoxy-1,3,5-triazin-2-yl) morpholinium chloride (DMT-MM) as condensing agent (Scheme 2). The uptake and intracellular distribution of the BODIPY-labelled LacCer analogues **11** and **12** were examined by confocal microscopy in PC12D cells – a line derived from a pheochromocytoma of the rat adrenal medulla – and it was stated that they accumulate in the Golgi apparatus.

LacCer **12** was labelled with the commercially available iTRAQ 113, *via* Cu-catalysed azide–alkyne cycloaddition, leading to derivative **13**. MS/MS spectrum showed a series of product ions corresponding to the rupture of interglycosidic linkages, together with the reporter ion, giving good information about the quantitative differential analysis of GSL samples based on the use of iTRAQ. Furthermore, BODIPY-labelled LacCer **9b** (depicted in Scheme 1) was incubated into PC 12D cells and it was observed that **9b** remains about 10 min on the plasma membrane before its transformation in different GSLs. Changes in the GSL patterns of cellular differentiation states and quantification of the various GSLs were achieved by nano-liquid chromatography (LC)-fluorescence detection (FLD)-electrospray ionisation (ESI)-mass spectrometry (MS).[36]

Globotriaosylceramides (Gb_3s), such as compound **14** in Scheme 3, are one of the targets of Shiga toxin (STx), a bacterial toxin responsible for pathogenicity of enterohemorrhagic *Escherichia coli*. In various cell types, several Gb_3s have been identified, differing for the length and nature (saturated or unsaturated) of the fatty acid chain (R = $C_{16:0}$, $C_{22:0}$, $C_{24:1}$ in compound **14**) and it has been suggested that the pathogenic behaviour of STx can be connected to variability of the ceramide skeleton bearing different fatty acid residues. To investigate on the relationship between Gb_3 structural nature and their role in the outcome of the disease, various BODIPY-labelled Gb_3s have been synthesized, as depicted in Scheme 3, with long pegylated chains, to avoid alteration in the binding properties to STx, in particular its subunit B (STxB).[37] The commercially available BODIPY probe **15** has been attached to the 2-OR long chain of the middle galactose moiety of GB_3s **14**, by click-chemistry. Gb_3 sphingolipids reside mainly in the plasma membrane, together with sphingomyelin (SM) and cholesterol, in glycoprotein lipid microdomains called lipid rafts. It seems that lipid rafts influence plasma membrane fluidity and protein trafficking and, therefore, are somewhat

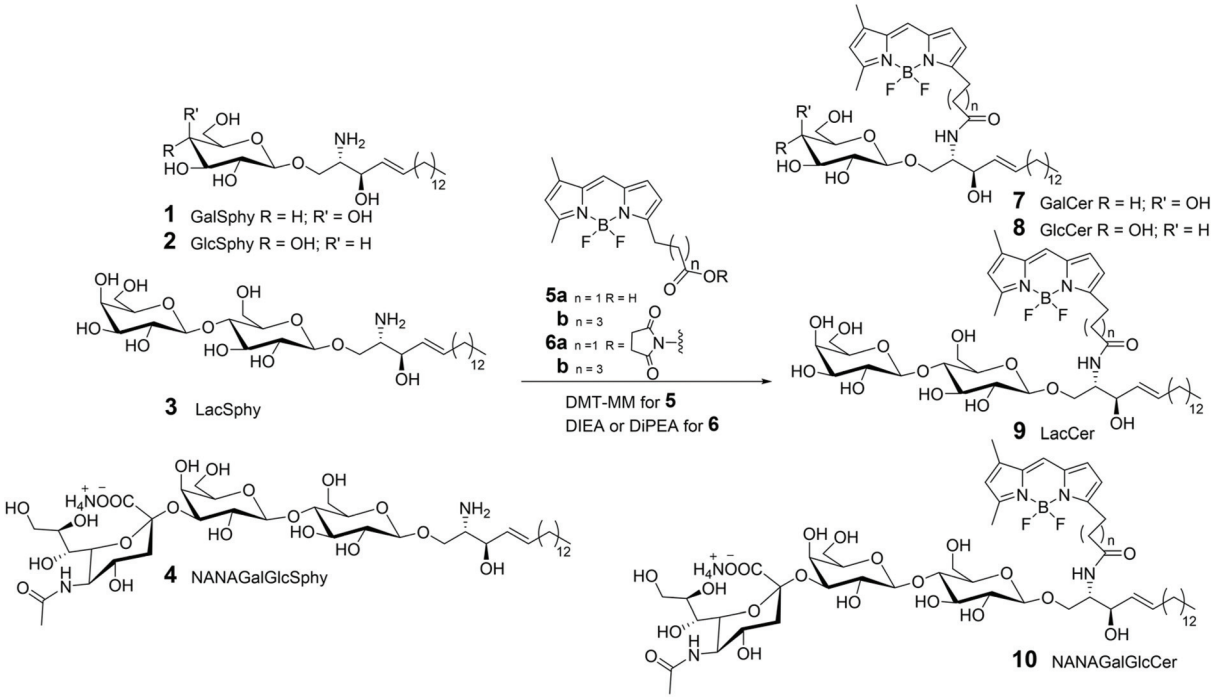

Scheme 1

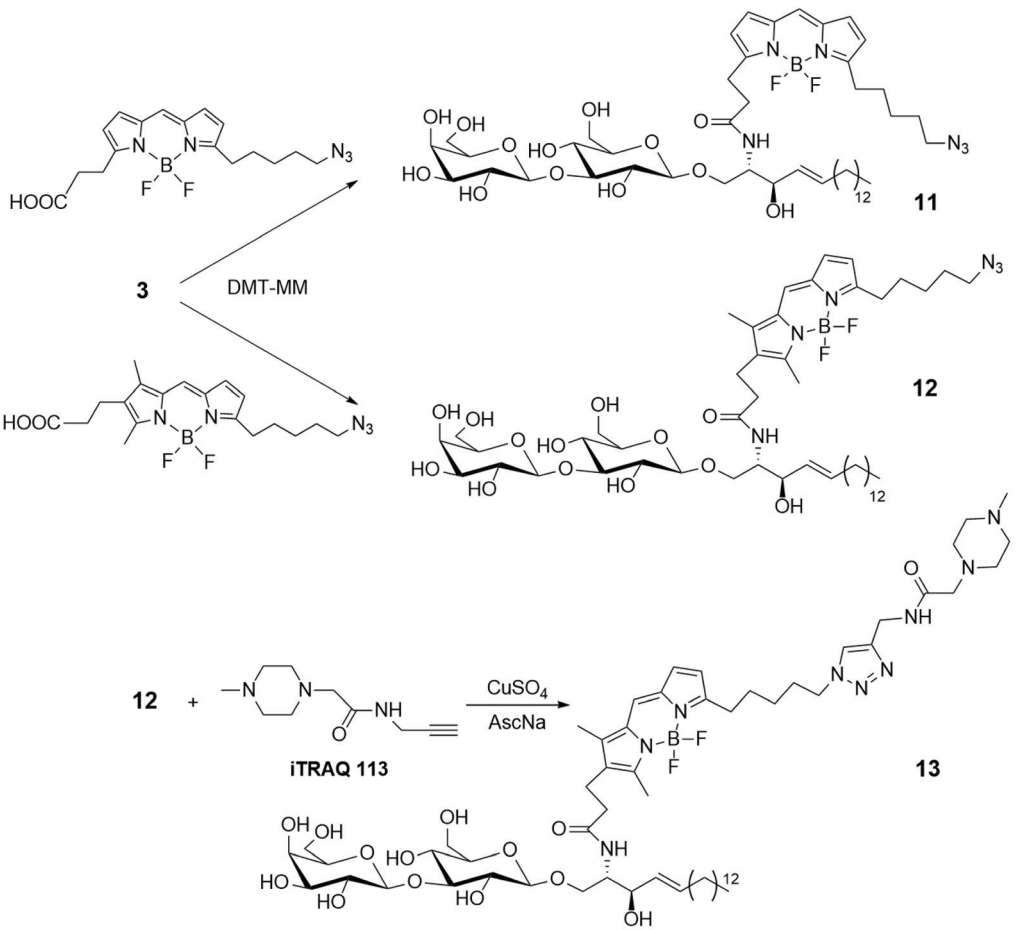

Scheme 2

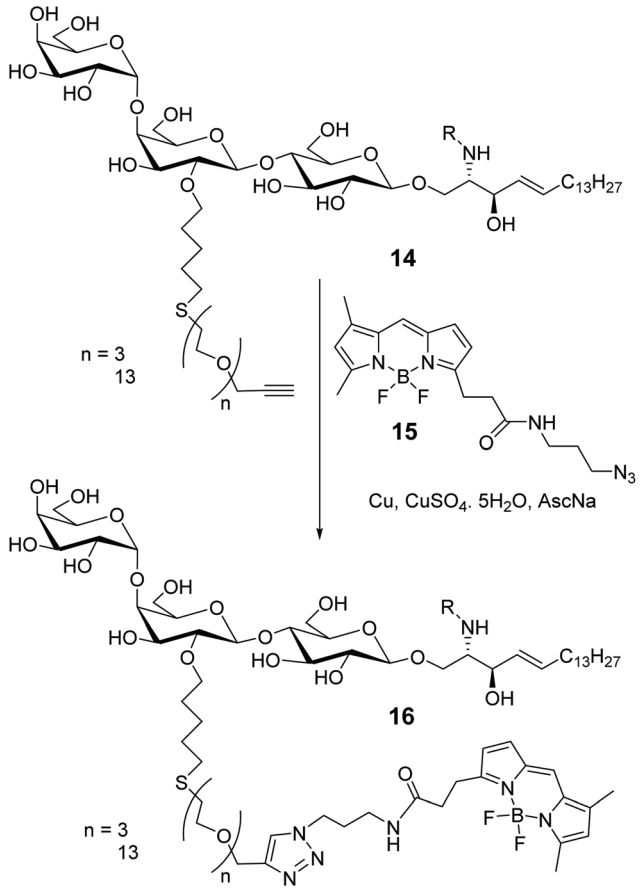

Scheme 3

involved in the signal transduction. To shed light on the nature and role of these domains, artificial giant unilamellar vesicles (GUVs), which incorporate glycosphingolipids **16**, were prepared to mimic plasma membrane vesicles, concluding that the fatty acid composition of Gb_3 lipids strongly influences the membrane reorganization of STx toxin that leads to the invagination of protein into the host cell.

BODIPY-glycosyl targeting probes

Among the various important characteristics that a good small fluorescent probe must possess, the solubility is one indispensable requirement for its application in the biological field.[38,39] Therefore, the lipophilic skeleton of BODIPY, that guarantees a certain cellular membrane permeability, has been opportunely modified with hydrophilic functionalities, such as carboxylic acid[40] or ammonium group,[41] or grafted to water-soluble carbohydrates[42] or polyethylene glycol,[43] or further linked to targeting groups, to penetrate the cellular membrane and visualize biomolecules in the cytosol and in specific organelles of cells.[44] In particular, the conjugation of a carbohydrate moiety to the BODIPY significantly improves the selectivity of the imaging probe towards a specific biological target. The presence of only one sugar linked to a BODIPY unit makes the fluorescent probes not only water-soluble but also able to penetrate the cell membrane, in some cases with a precise endocytosis mechanism.[45]

In Scheme 4 the most popular synthetic routes to BODIPYs **18** are shown. Furthermore, the Knoevenagel condensation of 3,5-dimethylBODIPYs with aromatic aldehydes provides direct entry into BODIPYs **19** and **20** that have redshifted fluorescence (NIR) properties.

Scheme 5 describes, instead, the most common methodologies for binding BODIPY derivatives to carbohydrates. The Cu(I)-catalyzed azide–alkyne 1,3-dipolar cycloaddition (CuAAC), a variant of the Huisgen cycloaddition, represents certainly the most popular way to graft BODIPYs to sugars, and its popularity resides in the fact that the azido and alkyne moieties can be placed either at the BODIPY core or at the glycosyl derivative and that the created triazole cycle is tolerated by the biological environment. On the other hand, the strain-promoted azide–alkyne cycloaddition, another variant of the Huisgen cycloaddition, is a powerful tool of bioorthogonal chemistry to study structure and function of biomolecules and cellular manipulations within living systems.[46] The cycloaddition, that has been elaborated avoiding the use of toxic Cu(I) catalyst, can proceed selectively and efficiently under physiological conditions, with fast kinetics, tolerance of aqueous environment and without biological side reactions.

Koenigs–Knorr-type or BF_3OEt_2 catalyzed glycosylations are also classical methodologies applied to achieve BODIPY/carbohydrate link.

Following our initial interest on luminescent properties and photoinduced electron and energy transfer in multicomponent BODIPY species,[47–52] we were the first to introduce a Pd-catalyzed cross-coupling for connecting the alkynyl glycosyl moiety, such as **21** or **22** in Scheme 5, to the *meso*-iodophenyl substituted BODIPY **20b** (Scheme 4).[53] The Sonogashira coupling can be considered the most popular methodology to form sp^2–sp carbon–carbon bond between aryl or alkenyl halides and terminal alkynes. The low yields obtained with the classical version and the necessary of an environmentally friend form of such coupling, prompted us to use the copper-free Sonogashira reaction. Quaternarization of the amino groups in glycosyl BODIPYs **23** and **24**, depicted in Scheme 5, introduced positive charges to these fluorescent monosaccharides and enhanced water-solubility, without essentially changing the red-emitting properties of such probes.

Absorption and luminescence properties of **23** and **24** are constant, passing from acetonitrile to aqueous solution. For both species, the emission and absorption spectra are shifted to a higher energy than for species **20b** (see Fig. 1), due to a partial charge transfer (CT) contribution in the latter, which drops out in **23** and **24** as the nitrogen lone pair is engaged with a methyl. Internalization experiments were conducted on African green monkey kidney (VERO) and THP-1 human monocytic (derived from an acute monocytic leukemia patient) cell lines, using a very low dyes concentration (1 nM), and no cytotoxic effect was observed up to 10 nM, suggesting that fluorescent probes **23** and **24** can be profitably used for biological

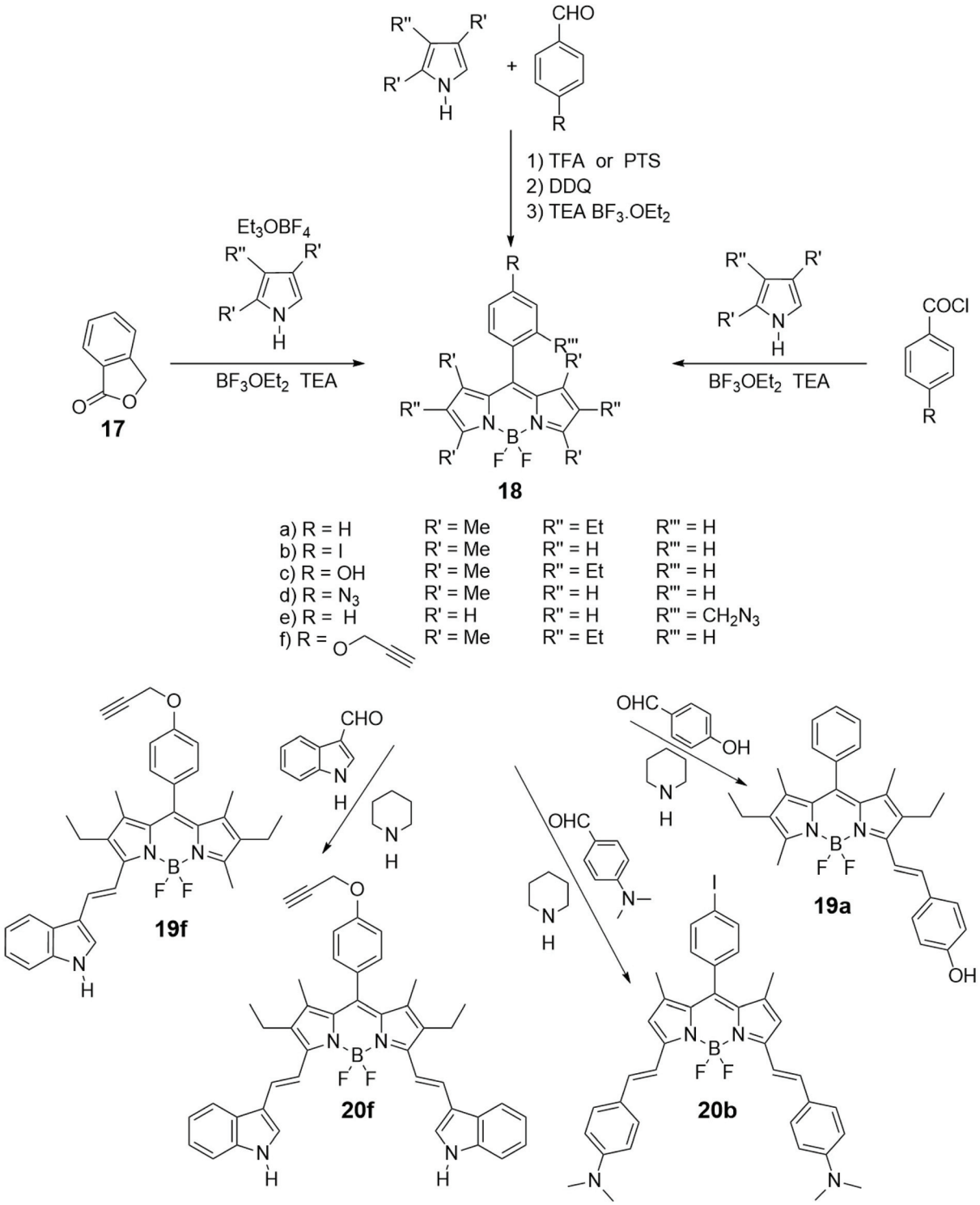

Scheme 4

investigations, see Fig. 2. Cell internalization mechanism was investigated and the presence of the sugar moiety seems to influence positively both biocompatibility and internalization pathway, that is mainly clathrin-dependent for probe 24 both for the non-tumour and tumour cell lines, whereas it appears much less clathrin-mediated for the less hydrophilic probe 23.[45]

Glycosylation of the phenolic functions of **18c** in Scheme 4 and **19a** (Scheme 5) was achieved with classical methodologies and, after deprotection, fluorescent probes **28** and **29**, depicted

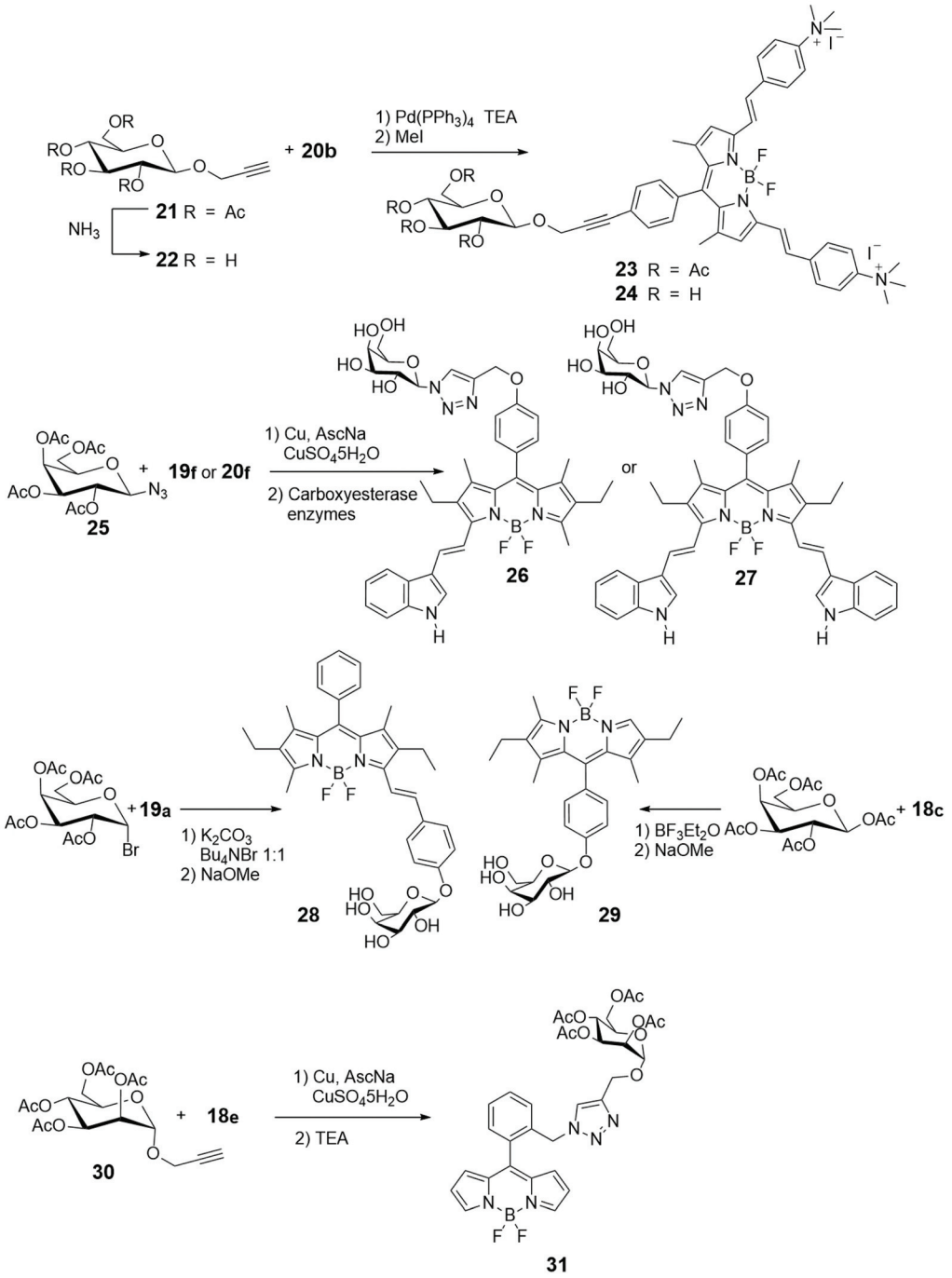

Scheme 5

in Scheme 5, were obtained and subjected, together with other BODIPY-labelled monosaccharides, to photodynamic therapy (PDT) studies on human lung cancer A549 cell lines.[54] Classical CuAAC conditions were used to link BODIPYs **19f** and **20a** to the commercially available azido galactose **25** shown in Scheme 5 and azido lactose derivative (not shown), and the fluorescent probes were deprotected by enzymatic cleavage.

Cellular uptake, cytotoxicity and intracellular localization of BODIPY-labelled monosaccharides **26** and **27** of Scheme 5 were investigated in human carcinoma Hep2 cells. No cytotoxicity was observed up to 10 mM of probe and deprotected probes were more efficient at cell internalization. These probes localized mainly in the endoplasmic reticulum of cells.[55] BODIPY-labelled mannose derivative **31** (depicted in Scheme 5) was prepared from azido BODIPY **18e** (Scheme 4) by CuAAC with sugar **30**. A complete study of fluorescence, lasing efficiency and photostability of these and similar probes are described.[56] One-pot procedure, briefly depicted in Scheme 4,

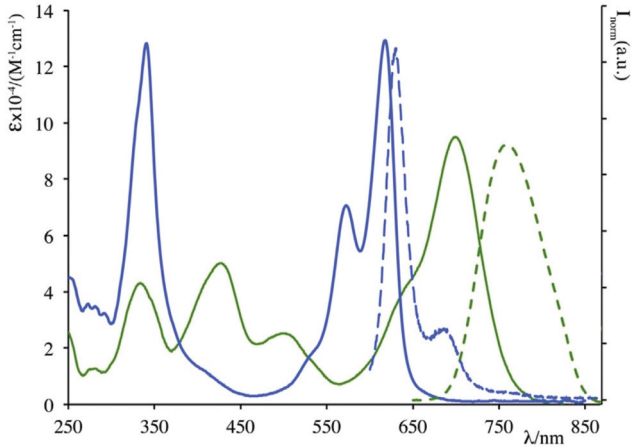

Fig. 1 Absorption (solid lines) and emission (dashed lines) spectra of **20b** (green) and **24** (blue) in acetonitrile solution.

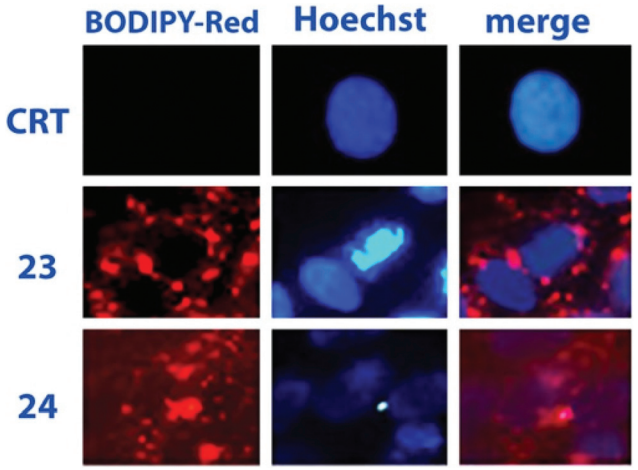

Fig. 2 Assessments of **23** and **24** internalization in VERO cells (dye concentration: 1 nM). Reproduced with permission from Elsevier.[42]

provides *O*-ethylation of phthalide **17** with Meerwein's reagent for the formation of a salt intermediate that reacts with pyrrole leading to *ortho*-substituted 8-C-aryl-BODIPYs, such as **18e** (Scheme 4).[57] A small library of water-soluble *ortho*-substituted BODIPY/carbohydrate conjugates with interesting photophysical and biological properties was recently synthesized.[58]

In an unusual synthetic procedure towards glycosyl BODIPYs,[59] the anomeric centre of mono-, di- and trisaccharides was used as reactive site for a pyrrole condensation, in the first step of the BODIPY skeleton synthesis (Scheme 6). The condensation opens the cyclic structure of the sugar, for example D-glucose (R = H), as shown in Scheme 6, from the anomeric carbon, without compromising the inherent chiral information. The monosaccharides lose their cyclic shape, turning into a hydroxylated chain linked to the BODIPY moiety, such as **32a**, whereas di- and trisaccharides preserve one or two rings, respectively, as in **32b–d**. The obtained BODIPY-labelled sugars were subjected to several derivatizations demonstrating the versatility of the synthetic procedure. All the compounds under study exhibited interesting absorption and emission properties, in accordance with those of the BODIPY scaffold. Confocal microscopy experiments on HeLa cells showed the easy cellular uptake, essentially in the cytoplasm, of such probes.

Microwave-assisted (MW) CuAAC reaction was used to link BODIPYs bearing azido or terminal triple bond, such as **33** in Scheme 7, to glycans possessing terminal alkyne or azido functions at the end of a pegylated chain.[60] Among others, glycosyl-BODIPY **34** in Scheme 7 readily underwent self-assembly into liposomes, when placed in water in the presence of phosphatidyl choline. Bright field and confocal microscopy confirmed liposome formation, the fluorescent emission of which was shifted from green to red when the concentration of compound **34** in liposomes increased.

Knoevenagel condensation of α-1-C-allyl glycosides **36** with **18d** (Scheme 4) led to the synthesis of the glycosyl-BODIPYs **37**, as shown in Scheme 8.[61] The azide-bearing BODIPY **18d**

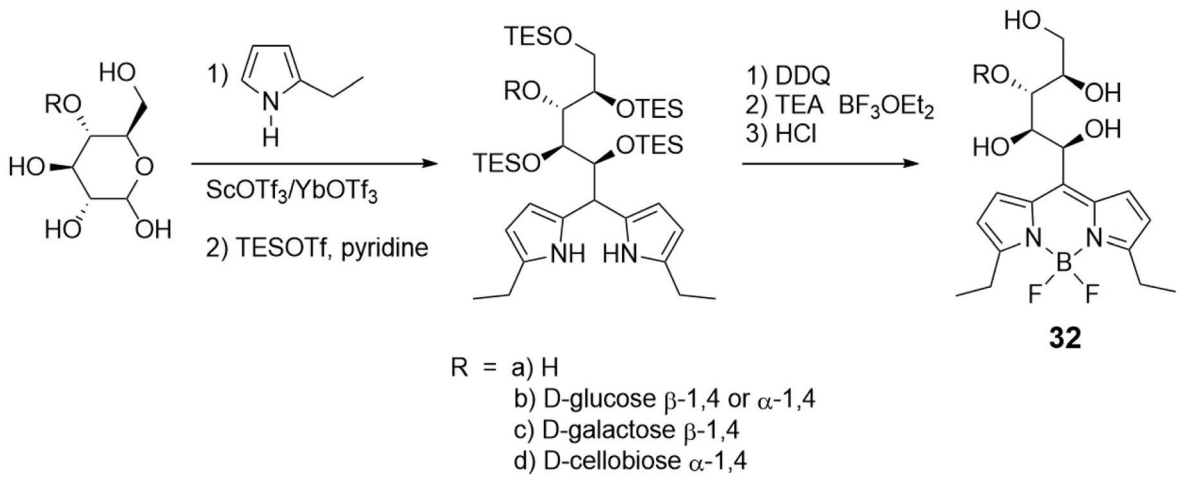

Scheme 6

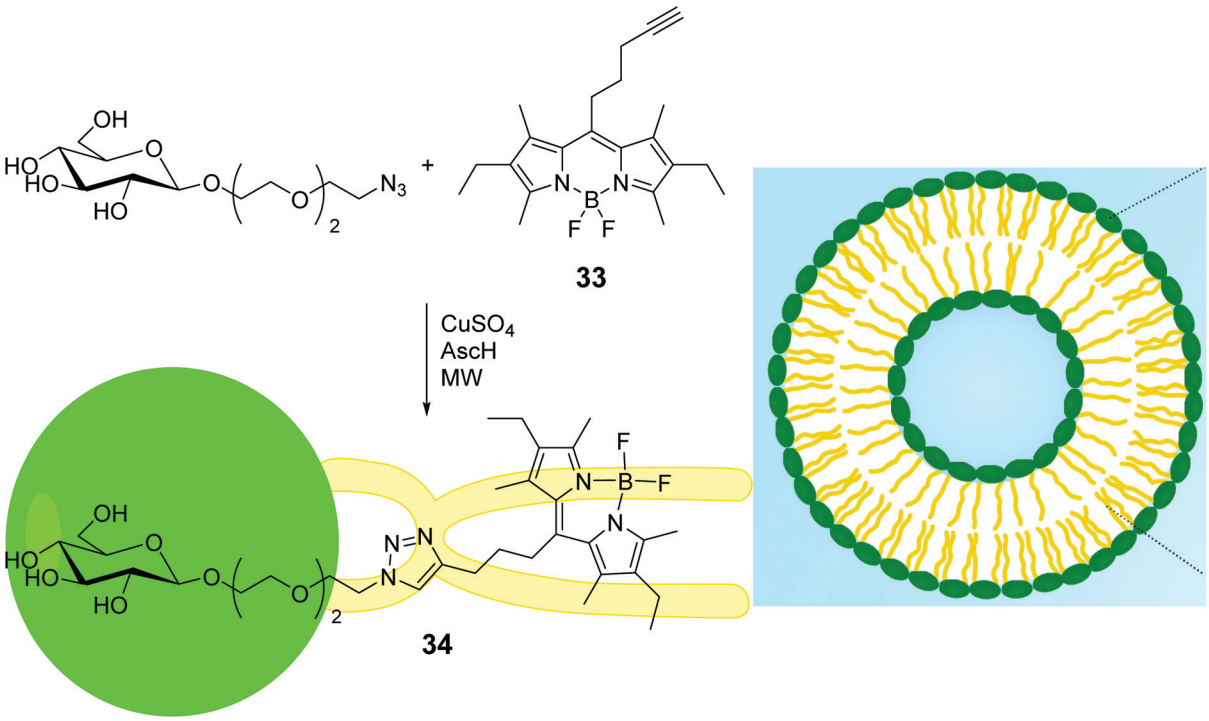

Scheme 7

was prepared using the mechanochemical approach,[62] which provides solvent-free conditions, as shown in Scheme 4. Glycosides **36** were obtained by a ligand-free Heck-type coupling, starting from mannose and glucose derivatives **35**, and the final deprotection of the sugar moieties afforded glycosyl-BODIPYs **37**. The two fluorescent probes were synthesized for dendritic cell-specific intercellular adhesion molecule-3-grabbing non-integrin (DC-SIGN) super-resolution bioimaging. DC-SIGN is a human lectin which shows a dual biological role of modulator of immune responses and as entry receptor for some pathogens, promoting the development of infections. The glycosyl-BODIPYs **37** (Scheme 8) displayed useful optical properties. The mannosyl-BODIPY **37b** was recognized by mannose-binding lectins in solid-phase immuno-assay (ELISA). It was also efficiently taken up by immune cells expressing DC-SIGN receptor, as proved by *in vitro* cellular investigations using fluorescence. Super-resolution stimulated emission depletion (STED) microscopy, allowed localization of **37b** in a densely crowded interior of immature dendritic cells (Fig. 3).

Most of the carbohydrate binding proteins are aggregated into oligomeric structures of high order,[63] and multivalent saccharide ligands were prepared considering them to be more effective than monosaccharide ligands (the cluster glycoside effect) in interacting with such macrostructures. Usually, the synthesis of multivalent saccharide ligands foresees polymeric or dendritic backbones or liposomes that display carbohydrate at the periphery of the macromolecules core. However, several multivalent saccharide ligands, not properly classified as macromolecules, demonstrated their efficacy. Recently, the preparation of an iminosugar cluster based on a BODIPY core and its photophysical properties were described. Iminosugars are mainly known to be inhibitors of a variety of carbohydrate-processing enzymes and some of them represent the first examples of multivalent iminosugars acting as pharmacological chaperones in the treatment of Gaucher disease, the most common lysosomal storage disorder. A fluorescent multifunctionalized BODIPY was used as backbone to link iminosugar derivatives, *via* azide–alkyne cycloaddition, leading to the formation of compounds **38** (Fig. 4). The anion of the dye commonly used for quantifying chaperoning activities, 4-methylumbelliferone, was used for the evaluation of fluorescent multivalent cluster **38a** as potential pharmacological chaperone. The quantification was carried out by estimating, *via* Stern–Volmer plots, the dynamic quenching of the luminescence of umbelliferone by **38a**, thanks to suitable spectral overlap between the emission of 4-methylumbelliferone anion and the absorption of the BODIPY species.[64]

The synthesis of three glucosyl-substituted BODIPY derivative **39** (Fig. 4) and its analogues mono- and diglycosyl BODIPYs was recently reported.[65] All the synthesized BODIPYs showed absorption bands centred at *ca.* 525 nm and fluorescence emission bands at 535 nm, in DMSO solutions. Their dark and photo cytotoxicity were investigated in human carcinoma Hep2 cells, using a cell titer blue viability assay, and none of them was toxic to cells. The time-dependent uptake of such multivalent glucosides was evaluated at a concentration of 10 μM in Hep2 cells over a period of 24 h and compound **39**, bearing three glucose units, showed the highest uptake, suggesting that the glucose moieties enhance cell internaliz-

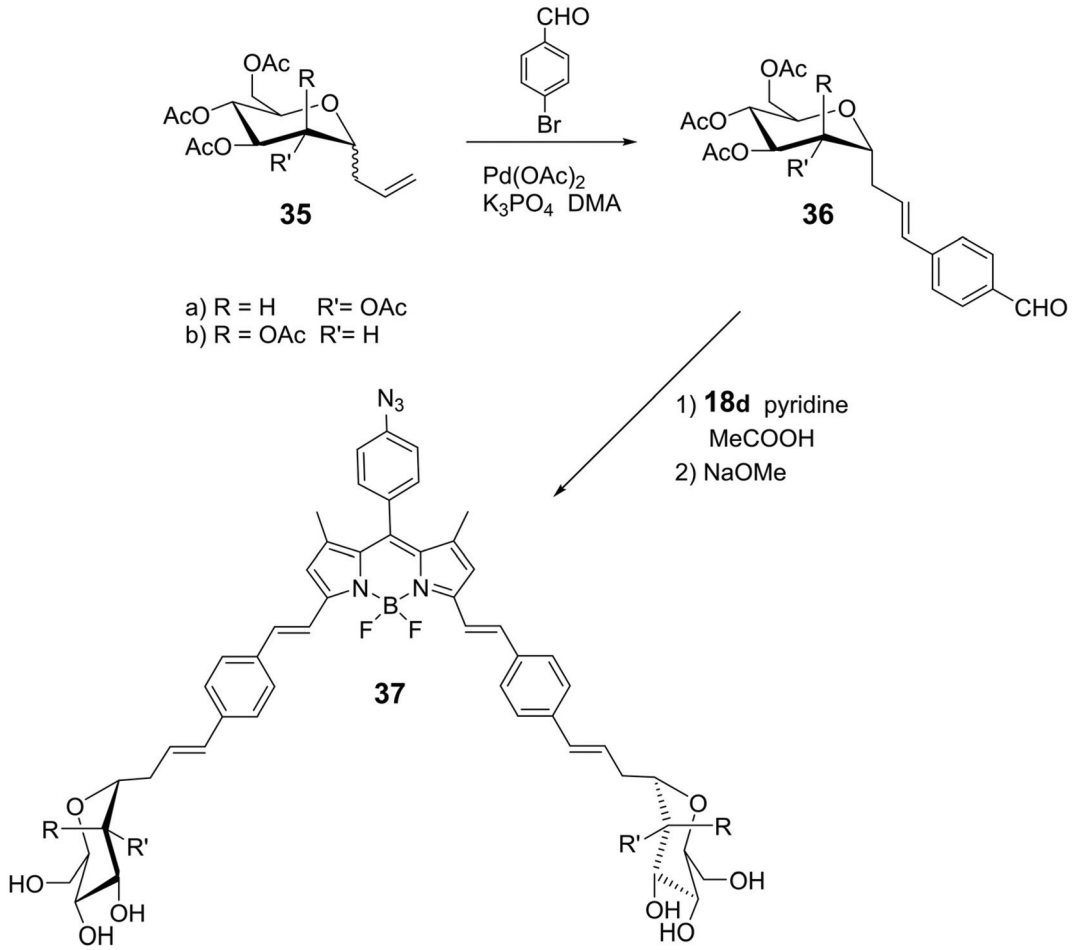

Scheme 8

ation, due to increased receptor-mediated recognition processes.

Enyne **40**, depicted in Scheme 9, is a derivative of the known dendritic ligand, based on the tetravalent pentaerythritol core, used for developing multivalent glycosides.[66] In its actual form **40** was subjected to a double glycosylation and cycloaddition with BODIPY **18e** (depicted in Scheme 4 and shown in Scheme 9) to lead to compound **41**.[67] Its reaction with the α-aminoacid **42** gave the fluorescent divalent mannoside **43**, while its dimerization and subsequent deprotection led to the BODIPY-labelled tetramannan derivative **44**, with boron–oxygen substitution, both obtained by a cross-metathesis approach. The spectral properties of such single and double BODIPY-labeled carbohydrate-based clusters **43** and **44** support their use as fluorescent markers.

The three-armed pegylated tri-azido BODIPY **45**, with iodine linked at the 2 and 6 positions of its skeleton, (Scheme 10) has been conjugated with three units of mannose **46**, *via* CuAAC. The mannosyl BODIPY **47** has been co-assembled with Tween 80, a non-ionic surfactant derived from polyethoxylated sorbitan and oleic acid, to form mannosyl BODIPY-loaded nanomicelles **48**. The cellular uptake of such nanomicelles was monitored by confocal laser scanning microscopy on MDA-MB-231 – breast cancer cells that overexpress mannose receptors (MR) – and human mammary MCF-10a cells with low MR expression. Results revealed a higher uptake of **48** by MDA-MB-231 cells with respect to BODIPY **47**, and its internalization *via* receptor-mediated endocytosis into cell lysosomes. After irradiation at 665 nm of MDA-MB-231 cells with nanomicelles **48** a significant change in their morphology was observed, indicating that **48** can function as a photosensitizer for photo dynamic therapy (PDT). Singlet oxygen was observed to disrupt lysosomal membrane and allowed the passage of assembled system **48** from lysosomes to cytoplasm, facilitating the assault of singlet oxygen to the other cellular organelles and the nucleus.[68]

Photoaffinity labelling (PAL) is a technique that exploit the photoexcitation of a labelling compound containing a photoactivable silent functional group. Once irradiated, the silent compound is converted in a reactive form that can irreversibly bind to a specific part of a macromolecule, like the active site of a protein. By the cross-linking of a labelling group, essential data about the structural and functional features of macromolecules can be recovered. Glucose or lactose decorated

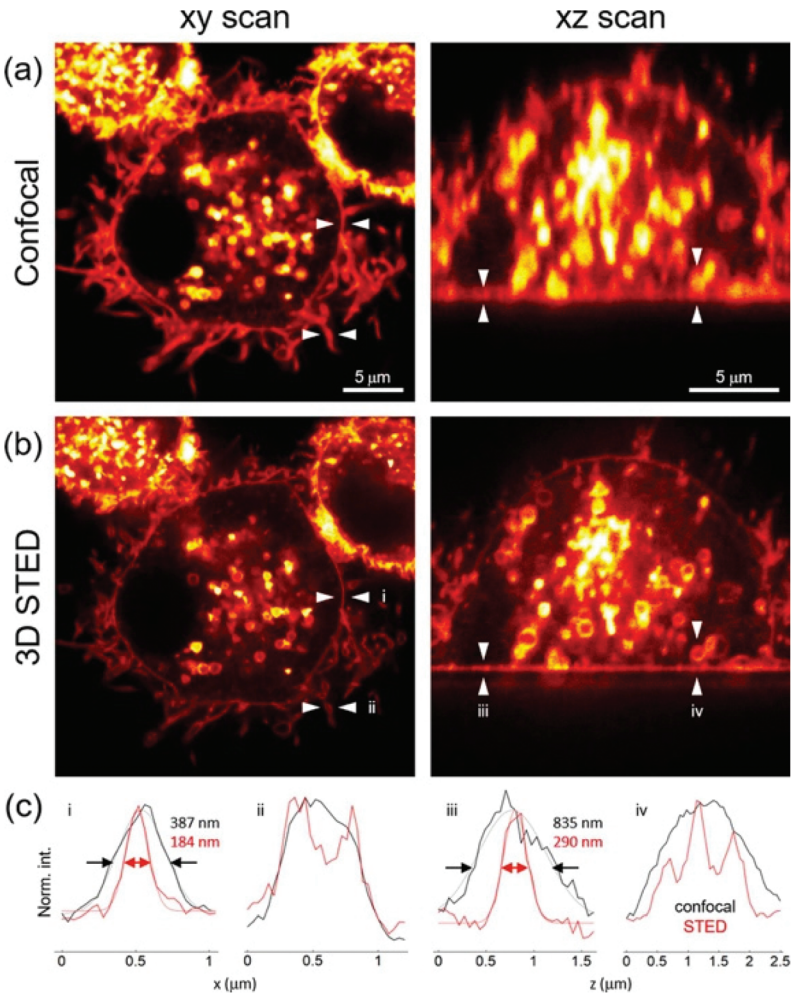

Fig. 3 Confocal and STED images (a and b respectively) of immature dendritic cells (iDCs) incubated with **37b**. Registered in lateral (*xy*, left) and axial cross-sections (*xz*, right); (c) intensity profiles extracted from the regions indicated with arrows, reproduced with permission from Elsevier.[61]

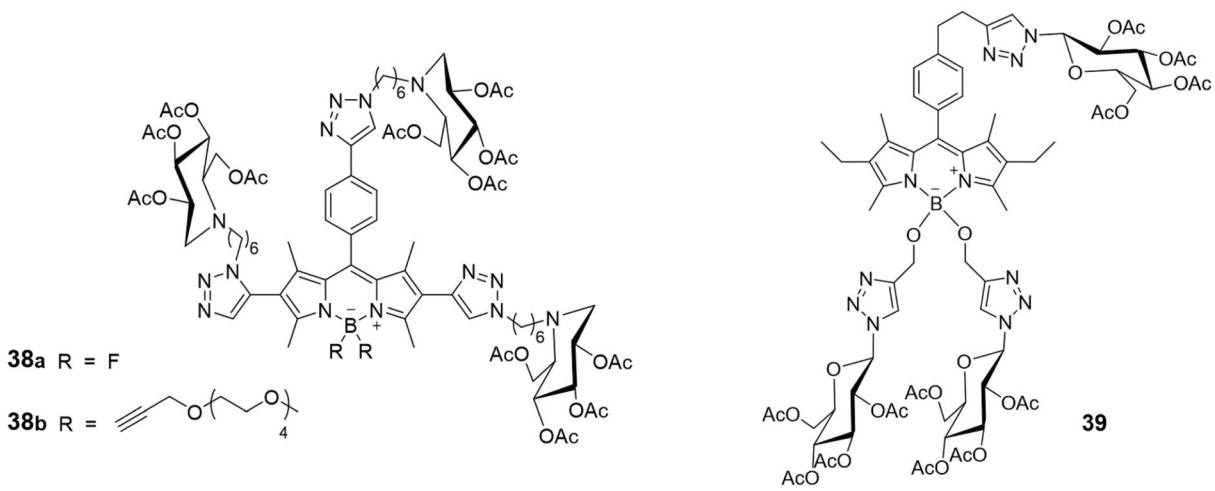

Fig. 4 Schematic representation of glucosyl-substituted BODIPY derivatives.

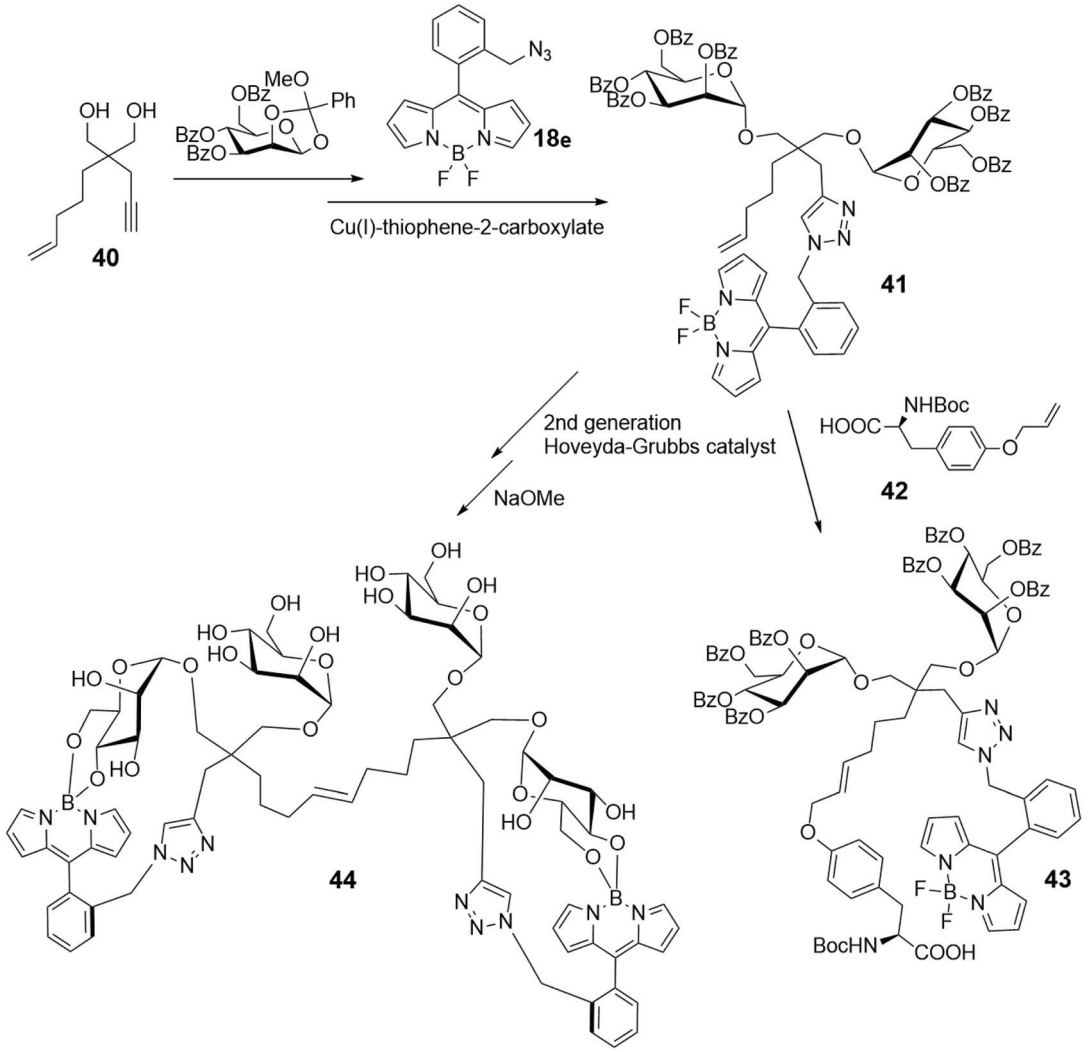

Scheme 9

photoaffinity probes were used for direct linkage with carbohydrate binding proteins, such as lactose-binding lectins. Their CuAAC with suitable BODIPY azides allowed the understanding of their action and/or behavior.[69] Lactose-based BODIPY fluorescent probes, bearing two different kind of photoreactive diazirine – alkyl and trifluoromethyl phenyl (TPD) functionalized – were synthesized to compare their reactivity and selectivity toward the peanut agglutinin (PNA).[70] The cycloaddition between the lactose derivatives **49** and the BODIPY **50** (Scheme 11) was the last step of the synthesis of the two PALs. They were then installed into PNA and the fluorescence intensity quantification was performed *via* sodium dodecyl sulfate polyacrylamide gel electrophoresis (SDS-PAGE) and subsequent fluorescence imaging. Furthermore, to compare the photo-crosslinking selectivity of TPD and alkyl diazirine probes, they were reacted with PNA mixed with proteins in HeLa cell lysate. TPD probe resulted the most efficient crosslinker with the target single binding protein, while the alkyl diazirine probe gave the best results in photoaffinity when reacted in HeLa cell lysate. A glucose moiety, instead of the lactose, was also used as head of two new probes.[71]

Cathepsins are enzymes (intracellular endopeptidases) present in animal tissues within lysosomes that play an important role in many pathology progressions like cancer, arthritis, Alzheimer disease and tissues degeneration.[72] Some of them are the cause of the decreasing of the anticancer response of the immune system, and others are implied in cell invasion. The use of specific markers has found to be of great impact for the analysis of the real role of cathepsins in the degenerative processes. A literature example of such approach is represented by system **51**[73] consisting of a BODIPY moiety (red) functionalized with two different groups having specific roles: an activity-based profiling probe (ABP), thebiotinylated peptide epoxysuccinate DCG-04 (green), known to be able to inhibit cysteine proteases, and a mannose cluster (black), exploited to selectively target lysosomes through mannose receptors (Fig. 5). The uptake of probe **51** by antigen presenting cells (APCs) and cathepsin labelling seems to proceed in a mannose-receptor depen-

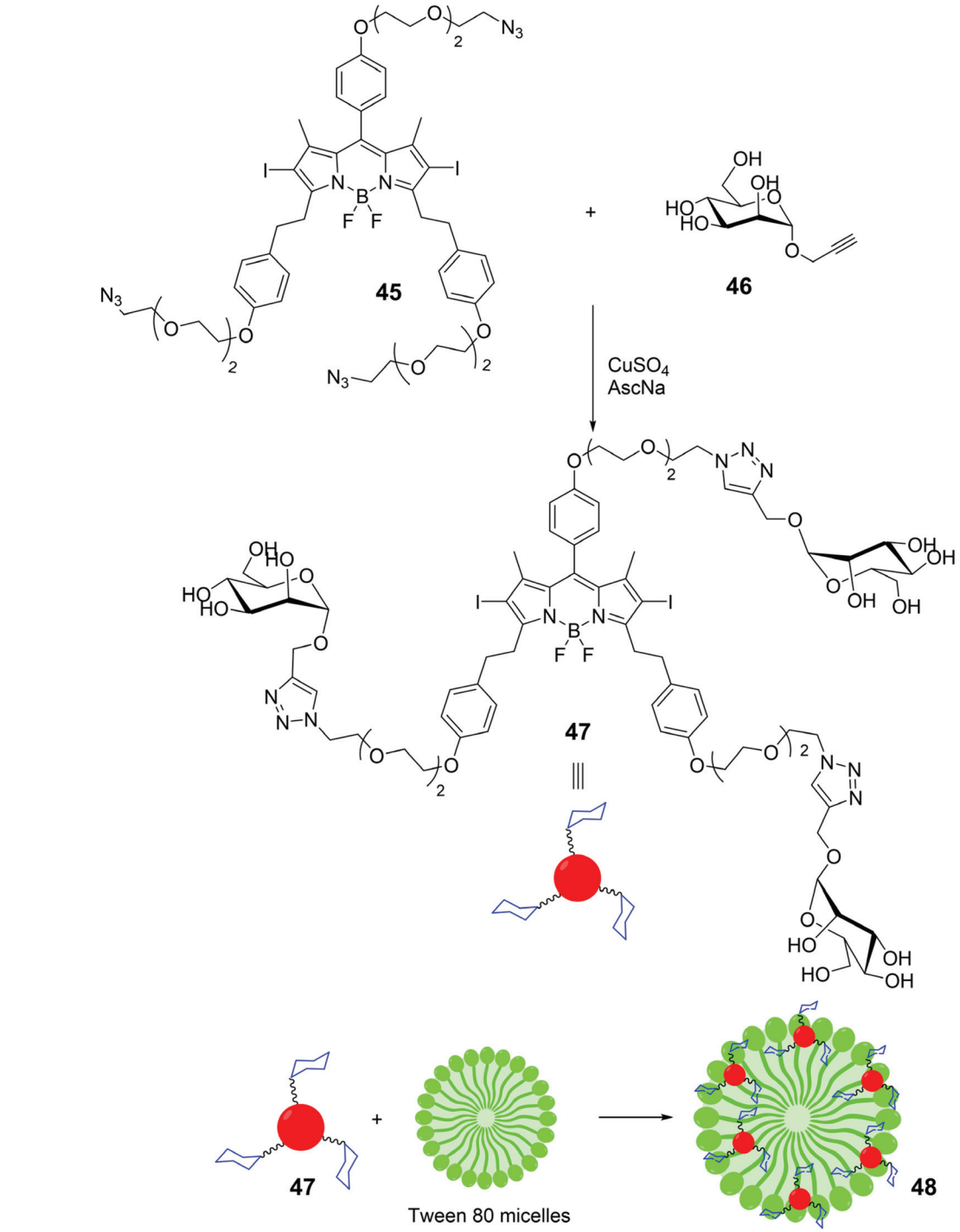

Scheme 10

dent manner. A different substitution at the *meso* position of the BODIPY moiety of compound **51** with an amino group[74] leads to new macromolecules that recognize the low pH (4.0–4.9) of the cathepsin-containing lysosomes. While at neutral or basic pH the fluorescence of these amino-BODIPY is quenched, the protonation of the aniline system at low pH restores the fluorescence. The modification of the complex probe structure of **51** with the inclusion of a phosphate moiety at the 6-position of the mannoside skeleton[75] causes massively different targeting abilities of these systems. Finally, the cellular uptake and inhibition towards cathepsins of the two triazole mannose clusters **52** and **53**, analogues to compound **51**, have been analyzed (Fig. 5). Results show that the amount of cathepsin inhibition depends on the saccharide dimension, the trisaccharide containing derivative **52** giving the best results with respect to the hepta-analogous **53**.[76]

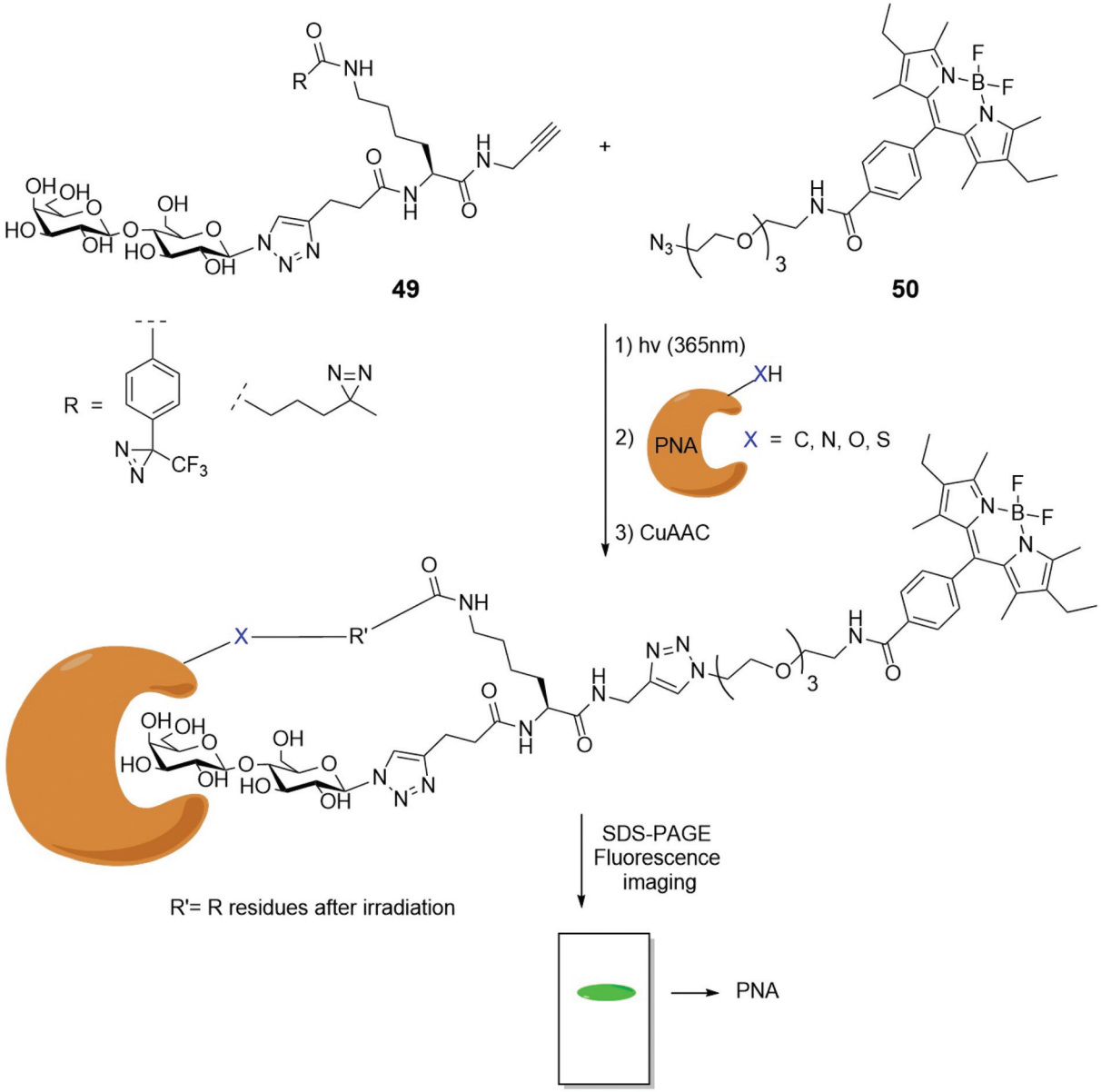

Scheme 11

Sialic acids (Sias), derivatives of neuraminic acid, are frequently found at the terminal position of the oligosaccharide moiety in glycoproteins and glycolipids are overexpressed and found at atypical levels in cancer tissues. Their mode of action is object of many studies, some of them employing fluorescent probes linked to the glycan structures or bioconjugating to them. To fully understand the role of cytidine 5′-monophosphate (CMP)-sialic acid in the transfer process of sialic acid moiety to glycans and the stages of its cellular pathway, the design and synthesis of a fluorescent probe (Scheme 12) were conceived, where a CMP-β-3″-F-Sia is linked through a PEG chain in 5″ position to a suitable, not charged, BODIPY skeleton.[77] After various challenging synthetic steps to obtain azide **54**, it was reacted with the cytidine phosphoramidite **55** to give, after phosphorous oxidation and DBU treatment, the CMP β-conjugation at sialic acid. The azido group of compound **56** was finally subjected to reduction by means of Lindlar catalyst, and the coupling with the succinimidyl ester of BODIPY-terminated hexaethylene glycol-yl propionic acid **57** led to the fluorescent probe **58**. Probe **58** was confirmed as potential inhibitor of N-2,3-STase from rat, and its uptake into isolated Golgi vesicles from rat liver (Sprague-Dawley rats) suggested that the compound was accepted as a substrate of CMP-sialic acid transporter.

Bio-orthogonal chemistry was also used for targeting sialic acids on cell surfaces. To understand the role of sialic glycans in several physiological and pathological events, a synthetic monosaccharide bearing a bio-orthogonal chemical reporter group was metabolically incorporated into the target glycan; the biochemically inserted group is able to react with a comp-

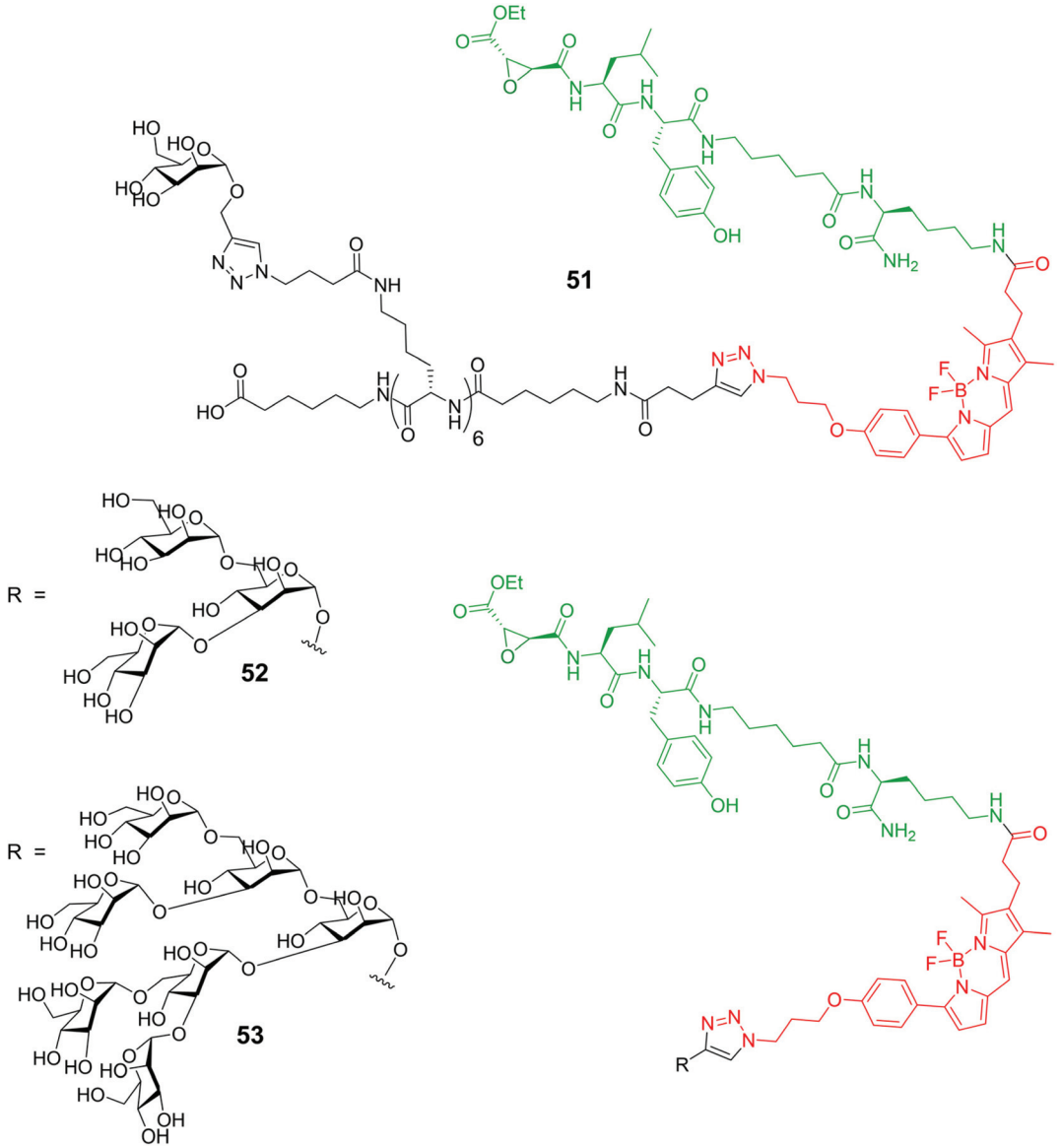

Fig. 5 Schematic representation of probes **51**, **52** and **53**.

lementary biorthogonal function linked to a fluorescent system.[78] The peracetylated derivative of mannose **59** in Scheme 13 was used as alkynyl reporter directed to sialic glycans. The choice of the BODIPY skeleton was made tacking into account that a pendant aryl moiety at a specific position of the probe can cause fluorescence-quenching *via* an acceptor-excited PeT (a-PeT) process. The low probe fluorescence could sensibly increase upon formation of the triazole derivative with the target glycan reporter group. For instance, BODIPY **60** (Scheme 13) was introduced in CL1-5 cells (lung cancer), cultured with peracetylated alkynyl-*N*-acetylmannosamine (Ac4ManNAl), by the strain-promoted azide–alkyne cycloaddition. The incorporation of alkyne tagged glycosyl conjugates in CL1-5 cells was visualized by confocal microscopy at very low concentration of **60** (0.1 μM), demonstrating that it enables cell imaging and visualization of glycoconjugates.

Similarly, *N*-azidoacetyl-mannosamine tetraacylated **61** (Fig. 6) was chosen as reporter molecule with the specific aim to quantify the Sias presence on tumour cell surfaces.[79] Cell surface Sias of SMMC-7721 (hepatocarcinoma cell) and LO2 (*para*-carcinomatous liver) were incubated with **61** and, subsequently, with the commercially available fluorescent dibenzocyclooctynyl-(polyethyleneglycol)$_4$-borondipyrromethene (DBCO-PEG4-BODIPY) **62** (Fig. 6). The on-cell-surface cycloaddition between Sias-azide moieties and DBCO-PEG4-BODIPY gave an emission signal directly connected with the Sias quantity. The cell surface Sias regulation under the administration of paclitaxel, a cancer drug, provided new insights in the drug functions and the biological role of the cell surface Sias in the related cancer metastasis processes.

Useful candidates for drug delivery and good probes for diagnostics are amphiphilic macromolecules able to self-

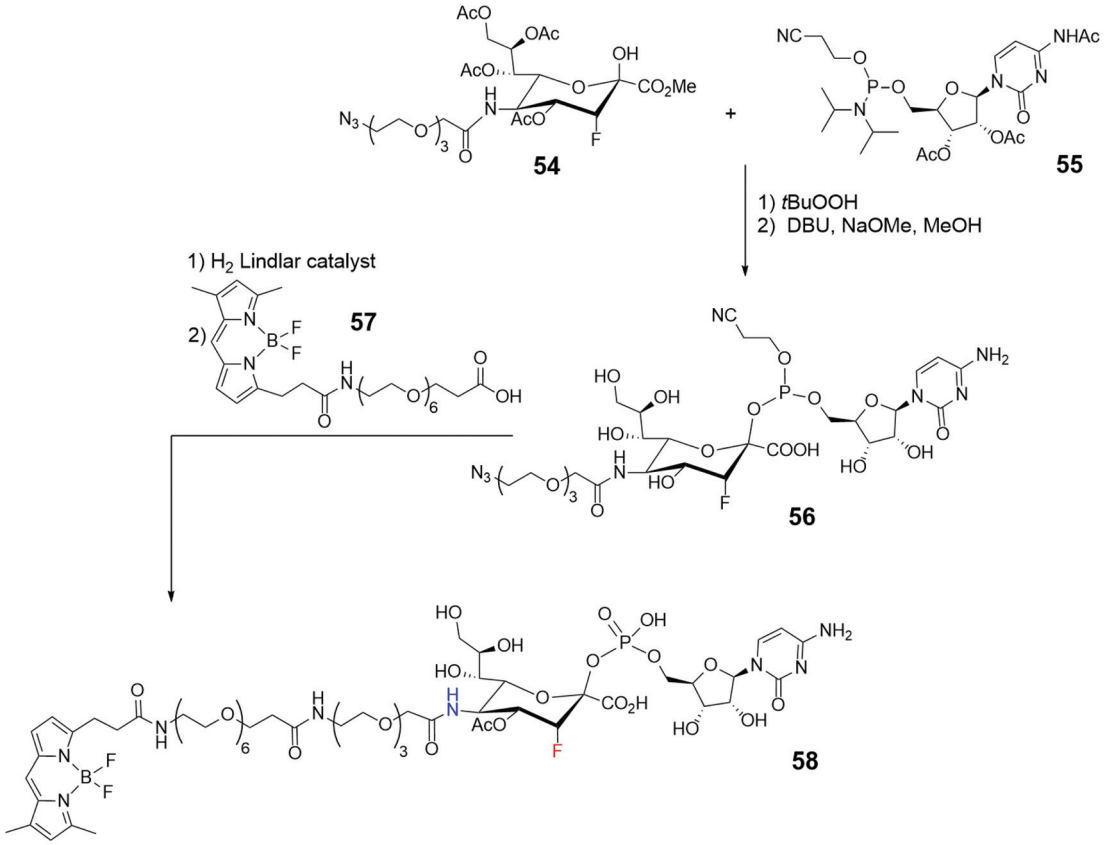

Scheme 12

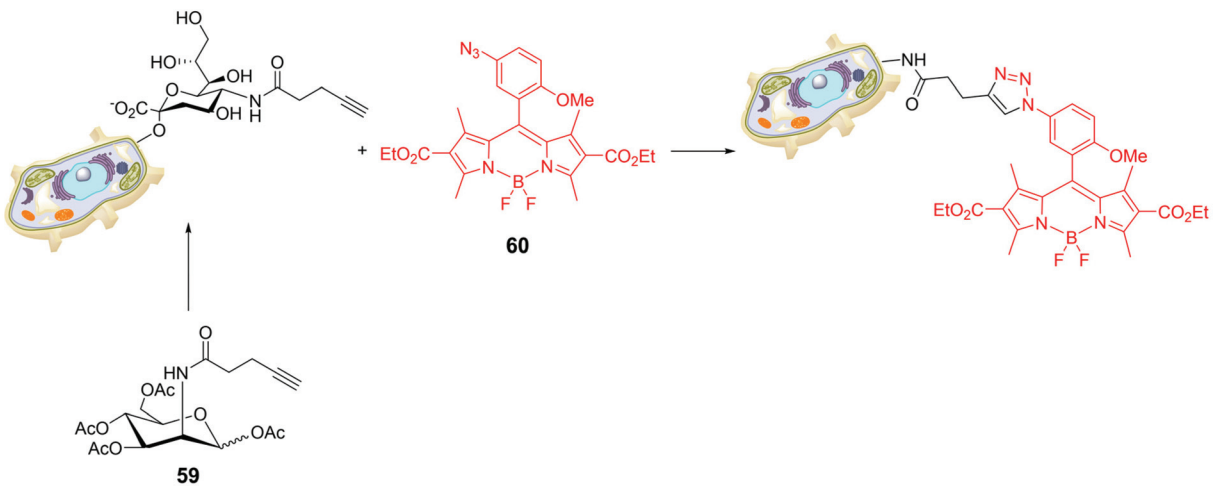

Scheme 13

assemble into nanometer-sized micellar systems. The key of these systems lies in the capacity of increasing permeability and retention (EPR) of micellar systems in the vascular structure of tumour tissue. These characteristics provide an inherent advantage for drug delivery applications, as the efficiency of the process depends essentially on the control of particle size. However, the absence of specificity and selectivity of such material does not lead to real accumulation in tumour zones, unless specifical targeting *via* ligand–receptor recognition.[80] Examples include ligand-like markers such as folic acid,[81] peptides,[82] antibodies,[83] and galactose.[84] Among others, galactose-functionalized polymers have been extensively adopted for this type of application. HepG2 cells (liver tissue immortal cells of Caucasian male with a well-differentiated hepatocellular carci-

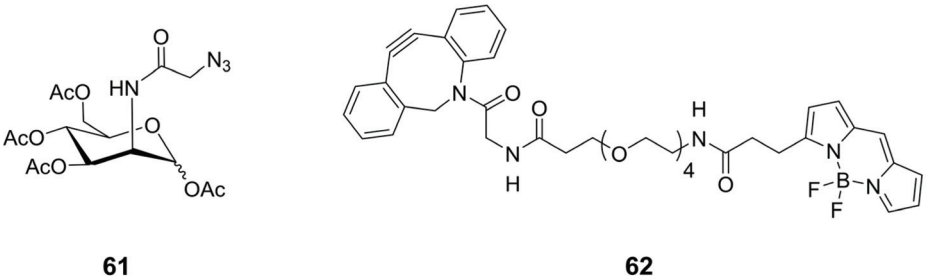

61 62

Fig. 6 Structures of *N*-azidoacetyl-mannosamine tetraacylated **61** and the commercially available dye **62**.

noma) are able to overexpress the galactose asialoglycoprotein receptor (ASGP-R) on their surface and therefore these polymeric nanomers can be rapidly received by HepG2.[85] The combination of the intrinsic properties of these substrates with the modulable photophysical characteristics of BODIPY led to the development of a glycopolymer device exhibiting near-infrared luminescence (NIRF).[86] The substrate, prepared *via* a multi-step reaction pathway (including ring-opening polymerisation and RAFT polymerisation), combines the recognition capabilities of galactose side chains with intense emission in the NIR region. In particular, the characteristic luminescence allowed to follow the endocytosis of HepG2 cells, demonstrating that NIRF glycopolymer self-assembled micelles are up-taken through a ligand–receptor recognition process. Therefore, this system containing galactose BODIPY subunits showed enhanced selectivity and cytotoxicity for hepatoma cells, exploiting a mechanism of ROS sensitisation, even at low light density. The fluorescence understanding makes this integrated system usable for NIR imaging by exploiting the selectivity and precision of the light input/output in this spectral region.

Position-specific incorporation of non-natural fluorescent amino acids in response to expanded codons has been shown to detect the activity and ligand-binding capacity of maltose-binding protein (MBP) through modulation of the fluorescence resonance energy transfer (FRET) process and fluorescence quenching, which is highly ligand-dependent.[87] Novel light-emitting protein probes can be also obtained by connecting fluorescent artificial amino acids and light-emitting proteins. Moreover, secreted reporters in the blood or serum have shown to be important tools for the detection, quantitation of different biological processes, *via* photophisical processes.[88] To this goal, *Gaussia luciferase* was linked to the C-terminus of a maltose binding protein and used as a BRET donor, while aminophenylalanine-modified BODIPY558 was incorporated into Tyr210, in a position vicinal to the maltose-binding site of the maltose-binding protein. In the system thus composed, a process of photoinduced energy transfer is active, which allows to observe not only the luminescence of the luciferase, but also the emission of BODIPY558. In the absence of maltose BODIPY558 emission is strongly quenched by a nearby tryptophan, but is recovered in the presence of maltose, which engages the tryptophan fragment.[89]

The synthesis of complex oligosaccharides is a process that involves lengthy and laborious protection/deprotection steps.[90] On the other hand, the enzymatic approach, which involves the use of glycosyltransferases (GTs), offers several advantages over purely chemical methods, due to the extreme stereo- and regiochemical control it provides.[91] The intrinsic limitation of this technique lies in its extreme selectivity and the limited availability of suitable enzymes. However, even if the field of protein engineering has evolved considerably, the attention towards GT has not been great, compared to other enzymes such as lipases, proteases and glycosidases. This is mainly due to the fact that selection processes for these types of enzymes work on micrometer scales and involve particularly high costs. The screening of large libraries would allow the analysis and engineering of much larger protein sequences. Fluorescence-activated cell sorting (FACS) is a special methodology within the field of flow cytometry.[92] FACS was originally developed to analyse protein–ligand interactions and only recently this methodology has been applied to the screening of enzyme libraries due to its sensitivity and speed of data accumulation.[93,94] A recent evolution of FACS, which takes advantage of the different physical properties of substrate and product, has been applied to the β-1,3-galactosyltransferare (CgtB), by using BODIPY as luminescent marker.[95] Sialyltransferase (ST) mutant gene libraries were expressed in *Escherichia coli* cells that are intrinsically permeable to an exogenous glycosyl acceptor (a BODIPY-lactose adduct, **63**) (Fig. 7).[95] Using this stratagem, the active STs that catalyses

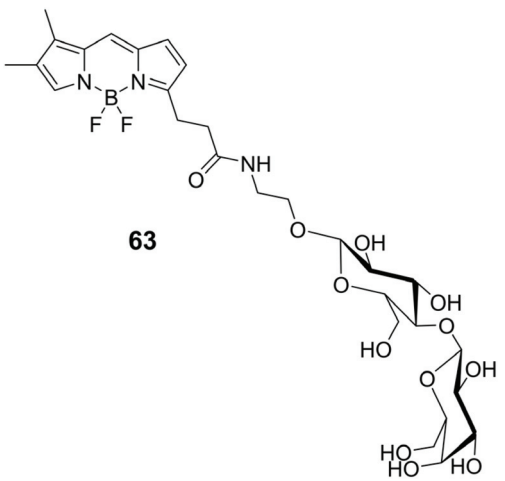

63

Fig. 7 The structure of the BODIPY-lactose adduct **63**.

the sialylation of fluorescent labelled lactose, trapping the fluorescent product within the cell allow co-localisation of genotype and phenotype. In this way, *Escherichia coli* cells are used as microreactors, allowing the use of millions of times smaller volumes of reagents than those required for robotic screening, resulting in huge cost savings.

BODIPY-based functional supramolecular sugar systems

Although carbohydrates have almost always been chosen as active subunits in structural recognition, or to enhance the solubility and modulate the polarity of fluorescent systems for molecular targeting, the presence of functionalizable groups and their size are particularly effective for assembling more than one photoactive subunit, resulting in functional supramolecular systems with modulable properties. As an alternative to what has been reported so far,[48–51] our approach to biocompatible glycosyl BODIPY probes involved the use of a sugar skeleton as scaffold, that retains the typical properties of a glycosidic fragment, and differently substituted BODIPY moieties, chosen to make changes to the photophysical properties of the entire systems.

We were the first to use the platform of a suitably functionalised glucose to build-up multiBODIPY molecular structures capable of functioning as artificial antenna systems exploiting photo-induced, extremely efficient and fast coulombic energy transfer. Copper-free Sonogashira cross-coupling was again elected to linking reaction between sugar and BODIPY moiety for its efficiency. Up to four propargyl moieties were introduced in the skeleton of methyl α-D-glucopyranoside to be connected, *via* the iodophenyl *meso*-substituent, to the BODIPY skeletons (Fig. 8). Dyad **1** consists of two BODIPYs with different electronic characteristics. The first one (shown in orange) absorbs visible light at around 500 nm and is characterized by luminescence with a very low stokes shift and quantum yields in the order of 60%, depending on the

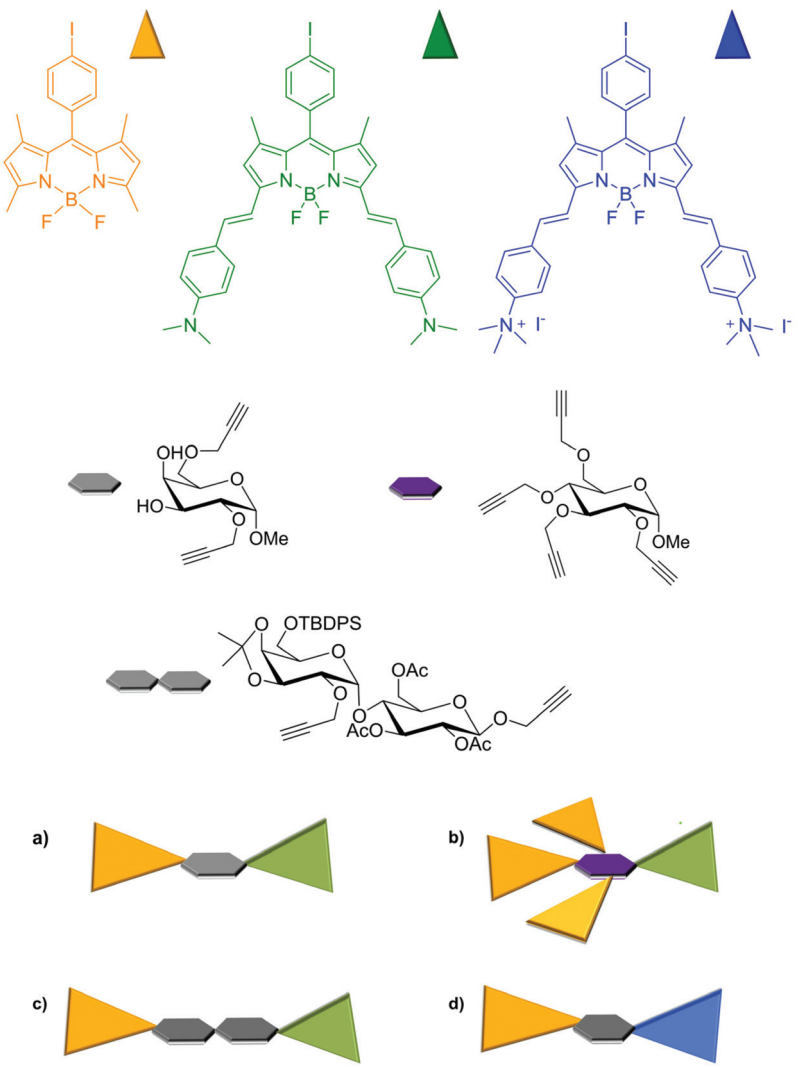

Fig. 8 Schematic representation of multicromophoric bodipy assembly on sugar scaffold.

solvent. The other BODIPY subunit (green in Fig. 8) exhibits a lower energy shifted absorption band, due to π–π* transitions, with a charge transfer contribution. The lowest-energy excited state of this subunit is luminescent in the NIR and is able to efficiently act as an acceptor of the energy absorbed by the orange subunit, keeping its electronic properties unchanged even when anchored to the sugar substrate. This type of behavior is particularly interesting for possible application in optical microscopy, as it allows luminescence to be observed in the red while exciting in the green or blue.

The energy transfer process in the antenna system **a** is extremely efficient and has been demonstrated, by pump–probe transient absorption spectroscopy, to occur in the order of 200 fs. The efficiency of the process remains almost unchanged in the analogous system **b** in which all hydroxyl functions of the sugar skeleton are engaged with BODIPY. In fact, by achieving even three donor subunits (orange BODIPY), leading to an increased cross section for absorption in the visible, light is completely transferred to the acceptor (green BODIPY) subunit, regardless of the distance imposed by the relative position of BODIPY moieties on the sugar scaffold. Besides, the presence of the monosaccharide assures the possibility of multifunctional systems such **a** and **b** to have application within the field of biologically relevant luminescent probes.[53]

In order to keep the sugar structure free from the encumbrance of chromophores and to study, in more details, the dependence of energy transfer efficiency on interchromophoric distance, we prepared dyads **c** in which the same BODIPY subunits were anchored on a disaccharide scaffold, see Fig. 8.[96] From a synthetic point of view, the construction of the disaccharide moiety was carried on using the well-known protection–deprotection chemistry proper of sugar synthesis,[97] anchoring to the disaccharide scaffold two triple bonds, one by glycosylation at the anomeric carbon of the glucosyl moiety and the other by functionalization of OH at the C-2 position of the galactosyl group. The linkage to the two BODIPYs was achieved once again adopting the copper-free Sonogashira coupling. Notably, the structural diversity of the isomeric multifunctional systems **c** did not affect the results of the photophysical studies conducted on them as mixture, since dyads **c** were perceived as a unique object with the two fluorescent units separated by the same distance in the space. The presence of the glycosidic scaffold, again, does not disturb their photophysical characteristics, as demonstrated by comparing the absorption spectra of the single chromophoric subunits with that of the dyad. Regardless of the excitation wavelength, this dyad also radiatively deactivates from the lowest-energy excited state located on the green BODIPY fragment, exhibiting luminescence at about 770 nm, in acetonitrile, similar to that exhibited by the green BODIPY. In this case, pump–probe spectroscopy experiments have clearly shown that the energy transfer process takes place at a rate of about 30 ps, with an efficiency of 99%, in spite of an interchromophoric distance of 24 Å. This result clearly shows that in addition to the distance, the main factor to be considered in the design and preparation of FRET systems is the spectral overlap between the absorption profile of the acceptor and the emission of the donor.[96]

In order to be effectively applied in the bio-imaging field, multichromophoric systems have to be designed to allow a large stokes shift, thus preventing scattered light effects in the fluorescence image recording, but a possible upgrade consists in introducing features that can influence the photophysical properties of these systems as a function of localization. To this end, we have recently shown that the introduction of positive charges on the scaffold of these dyads allows the modulation of energy transfer efficiency and emission color and intensity, depending on their position within a biological system.

Dyad **d**, shown in Fig. 8, was designed to contain two BODIPY subunits with again very different absorption and emission spectra.[98] A D-galactopyranoside, with two propargyl substituents at the OHs of C-2 and C-6 of the sugar moiety, respectively, was used as a bridge between the subunits, instead of the previously used D-glucopyranoside subunit. This choice was made for synthetic reasons, in particular, to facilitate the use of protecting groups during functionalization steps, since galactose-mediated inter-chromophoric interactions are very similar to those mediated by glucose. Further difference from the previously discussed multi-chromophoric systems lies in the quaternarization of the dimethylamino substituents of the BODIPY subunit previously shown in green (now blue in Fig. 8), quantitatively obtained by treating green BODIPY with an excess of methyl iodide in acetonitrile. Dyad **d** was completely soluble in water and therefore suitable for cellular studies. In this dyad the electronic energy transfer (EnT) between the components, from the high-energy dye (orange colored in Fig. 8) to the low-energy one (the blue unit in Fig. 8) occurs with high efficiencies (over 99%) in acetonitrile and leads to the radiative deactivation of the excited state of blue BODIPY with quantum yields, characteristic of this subunit,[97] in the order of 70%. In addition, the blue BODIPY subunit in Fig. 8 has absorption and emission properties that may be strongly dependent on the environment as consequence of its charge and the charge transfer nature of its excited states. Indeed, it has been shown that in aqueous solution this dyad organizes itself, reasonably protecting the lipophilic portion (orange BODIPY) and exhibiting the charged portion to the ambient. This behavior results in a very low quantum yield of luminescence from the blue BODIPY. The luminescence is switched on again in the presence of protein material (*e.g.* by addition of BSA), Fig. 9-top panel In the presence of a lipidic environment (*e.g.* oils) the system rearranges itself by protecting the charged portion and exposing the lipophilic one and the red emission is no longer observed, while the donor emission in the green portion of the electromagnetic spectrum becomes predominant, indicating that under these environmental conditions the energy transfer process is inefficient, see bottom panel in Fig. 9.

This behavior was confirmed in cellular environment, demonstrating that this dyad can illuminate different cellular compartments simultaneously and with different colors due to

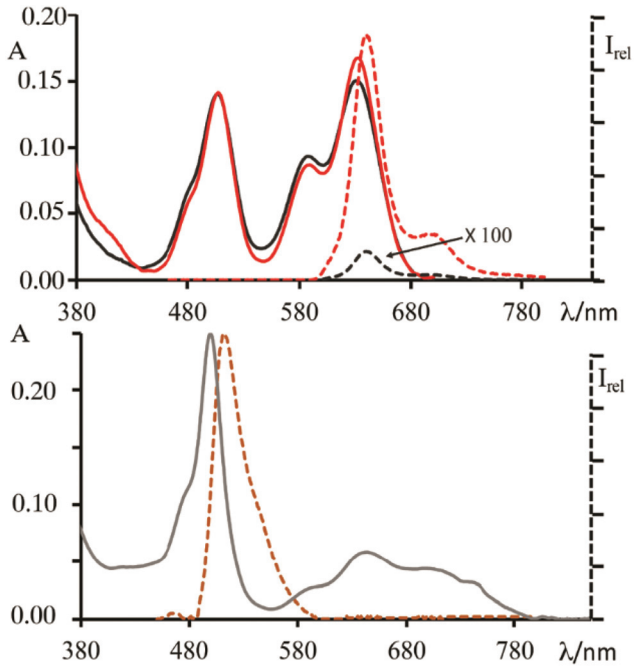

Fig. 9 Top: Absorption (black full line) and emission (black dashed line) spectra of 1 in PBS buffer solution; absorption (red full line) and emission spectra (dashed red line) registered after addition of 10 mg mL^{-1} of BSA to 2 mL PBS buffer solution of 1 ([1] = 5×10^{-6} M). Bottom: Absorption (grey line) and emission (orange line) spectra of 1 in oil ([1] = 5×10^{-6} M). Emission spectra were obtained upon excitation at 450 nm. Adapted from ref. 93 with permission of The Royal Society of Chemistry.

an effective modulation of the efficiency of photoinduced intercomponent EnT directed by the environment. A2780 cells (human ovarian cancer cells) treated with this species exhibit cytoplasmic luminescence in red (aqueous- and protein-rich environment) while illuminating lipidic droplets in green, see Fig. 10. The latter result is of particular interest in light of recent suggestions about the role of lipid droplets on cell health. Notably, the dual cell lightning was unchanged after 6 months of storage of the biological material at 4 °C. To complete the picture of the properties of this dyad with the potentiality of bioimaging probe, its antiproliferative activity was tested on various cell lines and it did not cause any trace of cellular suffering within the time of exposure necessary for imaging purposes.

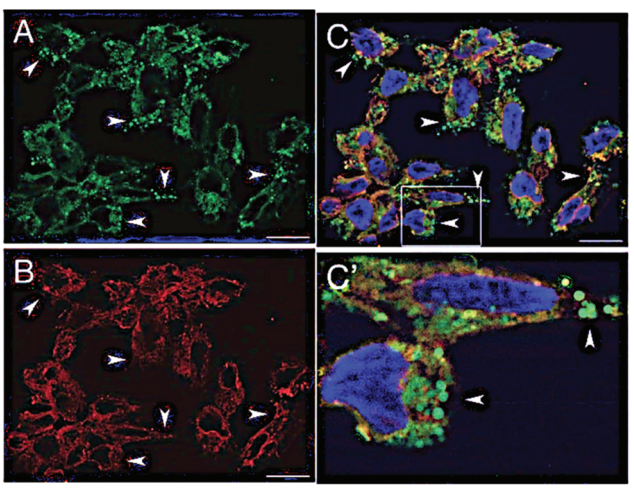

Fig. 10 Optical sections of A2780 cells incubated with 4 for 1 h and treated with paraformaldehide PFA (A–C) bar = 20 μm. Panel C′ show labeled cellular compartments at a higher magnification. Adapted from ref. 93 with permission of The Royal Society of Chemistry.

Conclusions and future perspectives

The complex structural world of carbohydrates combined with the modularity of BODIPY properties suggested the various uses that have been made of these two tools, both easily obtainable and modifiable. In this review we have described some of these uses pointing the reader attention to the synthetic approaches adopted for the linking of BODIPY to sugars and to the biological applications at cellular level, that have shown considerable *in vitro* results but still a low number of *in vivo* experiments. The labelling of carbohydrates to illuminate their path and learn about their functions was the first and most natural, although not trivial, use of the BODIPY/glycosides combination, followed by the synthesis of luminescent and targeting probes. The multi-functionalization of the sugar skeleton by BODIPY units differing in chemical–physical properties is a third alternative for the exploitation of their medical applications.

Future research work will be aimed at increasing the selectivity of multichromophoric BODIPY/glycosides systems within the cellular compartments, using chemistry to modify the BODIPY skeleton in order to adopt these species for *in vivo* imaging with luminescence shifted to the therapeutic window.

The synergic effect of the sugar fragment, that has been demonstrated to affect internalization cellular pathway and targeting towards specific cellular compartments, and the modulating properties of the excited states of BODIPY, depending on their structure, give significant chances to use these systems as sensitisers for the development of ROS and/or $^1O_2$ or in super-resolution microscopy such as STED.

The introduction of charges or glycoside fragments into BODIPY derivatives, where the lipophilic portion is greatly expressed, can make them structural components (photo- and redox-active) of liposomal structures, the function of which can be spent not just in drug delivery but possibly also in theranostic.

Conflicts of interest

There are no conflicts to declare.

Notes and references

1 R. A. Laine, *Glycobiology*, 1994, **4**, 759–767.
2 D. B. Werz, R. Ranzinger, S. Herget, A. Adibekian, C.-W. von der Lieth and P. H. Seeberger, *ACS Chem. Biol.*, 2007, **2**, 685–691.

3 L. Krishnamoorthy and L. K. Mahal, *ACS Chem. Biol.*, 2009, **4**, 715–732.
4 V. K. Tiwari, B. B. Mishra, K. B. Mishra, N. Mishra, A. S. Singh and X. Chen, *Chem. Rev.*, 2016, **116**, 3086–3240.
5 A. Mancuso, A. Barattucci, P. Bonaccorsi, A. Giannetto, G. La Ganga, M. Musarra-Pizzo, T. M. G. Salerno, A. Santoro, M. T. Sciortino, F. Puntoriero and M. L. Di Pietro, *Chem. – Eur. J.*, 2018, **24**, 16972–16976.
6 A. Barattucci, M. C. Aversa, A. Mancuso, T. M. G. Salerno and P. Bonaccorsi, *Molecules*, 2018, **23**, 1030–1042.
7 E. Deni, A. Zamarron, P. Bonaccorsi, A. Juarranz, F. Puntoriero, M. T. Sciortino, M. Ribagorda and A. Barattucci, *Eur. J. Med. Chem.*, 2016, **111**, 58–71.
8 M. Delbianco, P. Bharate, S. Varela-Aramburu and P. H. Seeberger, *Chem. Rev.*, 2016, **116**, 1693–1752.
9 X.-P. He, Y. Zang, T. D. James, J. Li, G.-R. Chen and J. Xie, *Chem. Commun.*, 2017, **53**, 82–90.
10 B. Thomas, K.-C. Yan, X.-L. Hu, M. Donnier-Maréchal, G.-R. Chen, X.-P. He and S. Vidal, *Chem. Soc. Rev.*, 2020, **49**, 593–641.
11 H. Yan, R. S. Yalagala and F. Yan, *Glycoconjugate J.*, 2015, **32**, 559–574.
12 L. Y. Niu, H. Li, L. Feng, Y. S. Guan, Y. Z. Chen, C. F. Duan, L. Z. Wu, Y. F. Guan, C. H. Tung and Q. Z. Yang, *Anal. Chim. Acta*, 2013, **775**, 93–99.
13 G. Ulrich, R. Ziessel and A. Harriman, *Angew. Chem., Int. Ed.*, 2008, **4**, 1184–1201.
14 A. M. Gomez and J. C. Lopez, *Chem. Rec.*, 2021, **21**, 3112–3130.
15 N. Boens, V. Leen and W. Dehaen, *Chem. Soc. Rev.*, 2012, **41**, 1130–1172.
16 M. S. T. Gonçalves, *Chem. Rev.*, 2009, **109**, 190–212.
17 S. Riela, A. Barattucci, D. Barreca, S. Campagna, G. Cavallaro, G. Lazzara, M. Massaro, G. Pizzolanti, T. M. G. Salerno, P. Bonaccorsi and F. Puntoriero, *Dyes Pigm.*, 2021, **187**, 109094–109101.
18 A. C. Benniston and G. Copley, *Phys. Chem. Chem. Phys.*, 2009, **11**, 4124–4413.
19 T. Papalia, R. Lappano, A. Barattucci, A. Pisano, G. Bruno, M. F. Santolla, S. Campagna, P. De Marco, F. Puntoriero, E. M. De Francesco, C. Rosano, M. Maggiolini and P. Bonaccorsi, *Org. Biomol. Chem.*, 2015, **13**, 10437–10441.
20 F. Cucinotta, B. P. Jarman, C. Caplan, S. J. Cooper, H. J. Riggs, J. Martinelli, K. Djanashvili, E. La Mazza and F. Puntoriero, *ChemPhotoChem*, 2018, **2**, 196–206.
21 N. Boens, B. Verbelen, M. J. Ortiz, L. Jiao and W. Dehaen, *Coord. Chem. Rev.*, 2019, **399**, 213024.
22 M. A. Filatov, *Org. Biomol. Chem.*, 2020, **18**, 10–27.
23 F. Nastasi, F. Puntoriero, S. Serroni, S. Campagna, J.-H. Olivier and R. Ziessel, *Dalton Trans.*, 2014, **43**, 17647–17658.
24 F. Nastasi, F. Puntoriero, S. Campagna, J.-H. Olivier and R. Ziessel, *Phys. Chem. Chem. Phys.*, 2010, **12**, 7392–7402.
25 E. Bassan, A. Gualandi, P. G. Cozzi and P. Ceroni, *Chem. Sci.*, 2021, **12**, 6607–6628.
26 R. Ziessel, G. Ulrich, A. Haefele and A. Harriman, *J. Am. Chem. Soc.*, 2013, **135**(30), 11330–11344.
27 M. Galletta, S. Campagna, M. Quesada, G. Ulrich and R. Ziessel, *Chem. Commun.*, 2005, **33**, 4222–4224.
28 J. Wang, N. Boens, L. Jiao and E. Hao, *Org. Biomol. Chem.*, 2020, **18**, 4135–4156.
29 E. Bassan, A. Gualandi, P. G. Cozzi and P. Ceroni, *Chem. Sci.*, 2021, **12**, 6607–6628.
30 P. De Bonfils, L. Péault, P. Nun and V. Coeffard, *Eur. J. Org. Chem.*, 2021, 1809–1824.
31 R. D. Singh, V. Puri, J. T. Valiyaveettil, D. L. Marks, R. Bittman and R. E. Pagano, *Mol. Biol. Cell*, 2003, **14**, 3254–3265.
32 V. Puri, R. Watanabe, R. D. Singh, M. Dominguez, J. C. Brown, C. L. Wheatley, D. L. Marks and R. E. Pagano, *J. Cell Biol.*, 2001, **154**(3), 535–547.
33 Y. Vo-Hoang, L. Micouin, C. Ronet, G. Gachelin and M. Bonin, *ChemBioChem*, 2003, **4**, 27–33.
34 O. C. Martin and R. E. Pagano, *J. Cell Biol.*, 1994, **125**, 769–781.
35 S.-H. Son, S. Daikoku, A. Ohtake, K. Suzuki, K. Kabayama, Y. Itoac and O. Kanie, *Chem. Commun.*, 2014, **50**, 3010–3013.
36 K. Arai, A. Ohtake, S. Daikoku, K. Suzuki, Y. Ito, K. Kabayama, K. Fukase, Y. Kanie and O. Kanie, *Org. Biomol. Chem.*, 2020, **18**, 3724–3733.
37 J. Sibold, K. Kettelhoit, L. Vuong, F. Liu, D. B. Werz and C. Steinem, *Angew. Chem., Int. Ed.*, 2019, **58**, 17805–17813.
38 N. Sabharwal, J. Chen, J. Lee, C. M. A. Gangemi, A. D'Urso and L. Yatsunyk, *Int. J. Mol. Sci.*, 2018, **19**, 3686–3703.
39 A. D'Urso, R. Randazzo, V. Rizzo, C. M. A. Gangemi, V. Romanucci, A. Zarrelli, G. Tomaselli, D. Milardi, N. Borbone, R. Purrello, G. Piccialli, G. Di Fabio and G. Oliviero, *Phys. Chem. Chem. Phys.*, 2017, **19**, 17404–17410.
40 H.-J. Zheng, W.-B. Chen, Z.-J. Wu, J.-G. Deng, W.-Q. Lin, W.-C. Yuan and X.-M. Zhang, *Chem. – Eur. J.*, 2008, **14**, 9864–9867.
41 P. Deng, F. Y. Xiao, Z. Wang and G. Jin, *Front. Chem.*, 2021, **9**, 89–99.
42 A. Baratucci, S. Campagna, T. Papalia, M. Galletta, A. Santoro, F. Puntoriero and P. M. Bonaccorsi, *ChemPhotoChem*, 2020, **4**, 647–658.
43 H. Wang, Y. Wu, P. Tao, X. Fan and G. C. Kuang, *Chem. – Eur. J.*, 2014, **20**, 16634–16643.
44 T. Kowada, H. Maeda and K. Kikuchi, *Chem. Soc. Rev.*, 2015, **44**, 4953–4972.
45 T. Papalia, G. Siracusano, I. Colao, A. Barattucci, M. C. Aversa, S. Serroni, G. Zappala, S. Campagna, M. T. Sciortino, M. T. Puntoriero and P. M. Bonaccorsi, *Dyes Pigm.*, 2014, **110**, 67–71.
46 J. M. Baskin and C. R. Bertozzi, *QSAR Comb. Sci.*, 2007, **26**, 1211–1219.
47 F. Puntoriero, F. Nastasi, T. Bura, R. Ziessel, S. Campagna and A. Giannetto, *New J. Chem.*, 2011, **35**, 948–952.

48 F. Puntoriero, F. Nastasi, S. Campagna, T. Bura and R. Ziessel, *Chem. – Eur. J.*, 2010, **16**, 8832–8845.
49 S. Diring, F. Puntoriero, F. Nastasi, S. Campagna and R. Ziessel, *J. Am. Chem. Soc.*, 2009, **131**, 6108–6110.
50 F. Nastasi, F. Puntoriero, S. Campagna, S. Diring and R. Ziessel, *Phys. Chem. Chem. Phys.*, 2008, **10**, 3982–3986.
51 T. Bura, F. Nastasi, F. Puntoriero, S. Campagna and R. Ziessel, *Chem. – Eur. J.*, 2013, **19**, 8900–8912.
52 A. Arrigo, G. La Ganga, F. Nastasi, S. Serroni, A. Santoro, M.-P. Santoni, M. Galletta, S. Campagna and F. Puntoriero, *C. R. Chim.*, 2017, **20**, 209–220.
53 P. Bonaccorsi, M. C. Aversa, A. Barattucci, T. Papalia, F. Puntoriero and S. Campagna, *Chem. Commun.*, 2012, **48**, 10550–10552.
54 N. Shivran, T. Mrityunjay, M. Soumyaditya, G. Pooja, S. Bhaskar, S. P. Birija and S. Chattopadhyay, *Eur. J. Med. Chem.*, 2016, **122**, 352–365.
55 T. Uppal, N. V. S. D. K. Bhupathiraju, M. Graca and H. Vicente, *Tetrahedron*, 2013, **69**, 4687–4693.
56 M. R. Martinez-Gonzalez, A. Urías-Benavides, E. Alvarado-Martínez, J. C. Lopez, A. M. Gómez, M. del Rio, I. Garcia, A. Costela, J. Bañuelos, T. Arbeloa, I. Lopez Arbeloa and E. Peña-Cabrera, *Eur. J. Org. Chem.*, 2014, 5659–5663.
57 M. del Río, F. Lobo, J. C. López, A. Oliden, J. Bañuelos, I. López-Arbeloa, I. Garcia-Moreno and A. M. Gómez, *J. Org. Chem.*, 2017, **82**, 1240–1247.
58 A. M. Gomez and J. C. Lopez, *Pure Appl. Chem.*, 2019, **91**, 1073–1083.
59 L. J. Patalag, S. Ahadi, O. Lashchuk, P. G. Jones, S. Ebbinghaus and D. B. Werz, *Angew. Chem., Int. Ed.*, 2021, **60**, 8766–8771.
60 R. S. Yalagala, S. A. Mazinani, L. A. Maddalena, J. A. Stuart, F. Yan and H. Yan, *Carbohydr. Res.*, 2016, **424**, 15–20.
61 G. Biagiotti, E. Purić, I. Urbančič, A. Krišelj, M. Weiss, J. Mravljak, C. Gellini, L. Lay, F. Chiodo, M. Anderluh, S. Cicchi and B. Richichi, *Bioorg. Chem.*, 2021, **109**, 104730–104739.
62 S. Fedeli, P. Paoli, A. Brandi, L. Venturini, G. Giambastiani, G. Tuci and S. Cicchi, *Chem. – Eur. J.*, 2015, **21**, 15349–15353.
63 J. F. Kennedy, P. M. G. Palva, M. T. S. Corella, M. S. M. Cavalcanti and L. C. B. B. Coelho, *Carbohydr. Polym.*, 1995, **26**, 219–230.
64 M. L. Lepage, A. Mirloup, M. Ripoll, F. Stauffert, A. Bodlenner, R. Ziessel and P. Compain, *Beilstein J. Org. Chem.*, 2015, **11**, 659–667.
65 A. L. Nguyen, K. E. Griffin, Z. Zhou, F. R. Fronczek, K. M. Smith and M. G. H. Vicente, *New J. Chem.*, 2018, **42**, 8241–8246.
66 J. J. Lundquist and E. J. Toone, *Chem. Rev.*, 2002, **102**, 555–578.
67 C. Uriel, R. Sola-Llano, J. Bañuelos, A. M. Gomez and J. C. Lopez, *Molecules*, 2019, **24**, 2050–2061.
68 Q. Zhang, Y. Cai, Q. Li, L. Hao, Z. Ma, X. Wang and J. Yin, *Chem. – Eur. J.*, 2017, **23**, 14307–14315.
69 K. Sakurai, S. Ozawa, R. Yamada, T. Yasui and S. Mizuno, *ChemBioChem*, 2014, **15**, 1399–1403.
70 K. Sakurai, T. Yasui and S. Mizuno, *Asian J. Org. Chem.*, 2015, **4**, 724–728.
71 K. Sakurai, T. Yamaguchi and S. Mizuno, *Bioorg. Med. Chem. Lett.*, 2016, **26**, 5110–5115.
72 A. Pišlar and J. Kos, *Mol. Neurobiol.*, 2014, **49**, 1017–1030.
73 U. Hillaert, M. Verdoes, B. I. Florea, A. Saragliadis, K. L. L. Habets, J. Kuiper, S. Van Calenbergh, F. Ossendorp, G. A. Van Der Marel, C. Driessen and H. S. Overkleeft, *Angew. Chem., Int. Ed.*, 2009, **48**, 1629–1632.
74 S. Hoogendoorn, K. L. Habets, S. Passemard, J. Kuiper, G. A. van der Marel, B. I. Florea and H. S. Overkleeft, *Chem. Commun.*, 2011, **47**, 9363–9365.
75 S. Hoogendoorn, G. H. M. van Puijvelde, J. Kuiper, G. A. van der Marel and H. S. Overkleeft, *Angew. Chem.*, 2014, **126**, 11155–11158.
76 C. S. Wong, S. Hoogendoorn, G. A. van der Marel, H. S. Overkleeft and J. D. C. Codee, *ChemPlusChem*, 2015, **80**, 928–937.
77 K. Suzuki, A. Ohtake, Y. Ito and O. Kanie, *Chem. Commun.*, 2012, **48**, 9744–9746.
78 J. J. Shie, Y. C. Liu, Y. M. Lee, C. Lim, J. M. Fang and C. H. Wong, *J. Am. Chem. Soc.*, 2014, **136**, 9953–9961.
79 Y. Liang, X. Jiang, R. Yuan, Y. Zhou, C. Ji, L. Yang, H. Chen and Q. Wang, *Anal. Chem.*, 2017, **89**, 538–543.
80 T. Xing, X. Yang, L. Fu and L. Yan, *Polym. Chem.*, 2013, **4**, 4442–4449.
81 M. Yu, L. Yutao and F. Si-Shen, *Biomaterials*, 2011, **32**, 4058–4066.
82 W. Su, H. Wang, S. Wang, Z. Liao, S. Kang, Y. Peng, L. Han and J. Chang, *Int. J. Pharm.*, 2012, **426**, 170–181.
83 C.-M. J. Hu, S. Kaushal, H. S. T. Cao, S. Aryal, M. Sartor, S. Esener, M. Bouvet and L. Zhang, *Mol. Pharmaceutics*, 2010, **7**, 914–920.
84 X. Cai, X. Li, Y. Liu, G. Wu, Y. Zhao, F. Chen and Z. Gu, *Pharm. Res.*, 2012, **29**, 2167–2179.
85 J. H. Han, Y. K. Oh, D. S. Kim and C. K. Kim, *Int. J. Pharm.*, 1999, **188**, 39–47.
86 L. Liu, Z. Ruan, T. Li, P. Yuan and L. Yan, *Biomater. Sci.*, 2016, **4**, 1638–1645.
87 I. Iijima and T. Hohsaka, *ChemBioChem*, 2009, **10**, 999–1006.
88 B. A. Tannous, *Nat. Protoc.*, 2009, **4**, 582–591.
89 A. Yamaguchi and T. Hohsaka, *Bull. Chem. Soc. Jpn.*, 2012, **85**, 576–583.
90 D. Wu, M. Fujio and C. H. Wong, *Bioorg. Med. Chem.*, 2008, **16**, 1073–1083.
91 C. A. Weijers, M. C. Franssen and G. M. Visser, *Biotechnol. Adv.*, 2008, **26**, 436–456.
92 A. L. Givan, *Flow Cytometry: First Principles*, Wiley-Liss, NY, 1992.
93 N. Varadarajan, S. Rodriguez, B. Y. Hwang, G. Georgiou and B. L. Iverson, *Nat. Chem. Biol.*, 2008, **4**, 290–294.
94 N. Varadarajan, G. Georgiou and B. L. Iverson, *Angew. Chem., Int. Ed.*, 2008, **47**, 7861–7863.

95 G. Yang, J. R. Rich, M. Gilbert, W. W. Wakarchuk, Y. Feng and S. G. Withers, *J. Am. Chem. Soc.*, 2010, **132**, 10570–10577.
96 T. Papalia, A. Barattucci, S. Campagna, F. Puntoriero, T. Salerno and P. Bonaccorsi, *Org. Biomol. Chem.*, 2017, **15**, 8211–8217.
97 S. G. Pistorio, S. A. Geringer, K. J. Stine and A. V. Demchenko, *J. Org. Chem.*, 2019, **84**, 6576–6588.
98 P. Bonaccorsi, T. Papalia, A. Barattucci, T. M. Salerno, C. Rosano, P. Castagnola, M. Viale, M. Monticone, S. Campagna and F. Puntoriero, *Dalton Trans.*, 2018, **47**, 4733–4738.